T.C.

MUĞLA SITKI KOÇMAN UNIVERSITY

GRADUATE SCHOOL OF NATURAL AND APPLIED SCIENCES

DEPARTMENT OF CIVIL ENGINEERING

SEISMIC RESILIENCE OF A SCHOOL BUILDING IN MILAS/MUGLA

MASTER OF SCIENCE

ZUBAIR SEDIQI

AUGUST 2021

MUĞLA

T.C.

MUĞLA SITKI KOÇMAN UNIVERSITY

GRADUATE SCHOOL OF NATURAL AND APPLIED SCIENCES

DEPARTMENT OF CIVIL ENGINEERING

SEISMIC RESILIENCE OF A SCHOOL BUILDING IN MILAS/MUGLA

MASTER OF SCIENCE

ZUBAIR SEDIQI

AUGUST 2021

MUĞLA

MUĞLA SITKI KOÇMAN UNIVERSITY

Graduate School of Natural and Applied Sciences

THESIS ACCEPTANCE APPROVAL

The thesis, submitted by **ZUBAİR SEDİQİ,** entitled **"SEISMIC RESILIENCE OF A SCHOOL BUILDING IN MILAS/MUGLA"** has been accepted on Day/Month/Year in fulfilment of master's degree in the Department of Civil Engineering by the thesis committee listed below.

THESIS DEFENCE COMMITTEE

Assist Prof. Dr. Ebru HARMANDAR (Head Of Committee)
Signature: Muğla Sıtkı Koçman University, Muğla

Assist Prof. Dr. Ebru HARMANDAR (Supervisor) Signature:
Muğla Sıtkı Koçman University, Muğla

Assist Prof. Dr. Osman KAYA (Member) Signature:
Muğla Sıtkı Koçman University, Muğla

Assoc. prof. Dr. Özkan KALE (Member) Signature:

Ted university, Ankara

DEPARTMENT APPROVAL

Prof. Dr. Recep Birgül (Head of Department) Signature:
Muğla Sıtkı Koçman University, Muğla

Assist Prof. Dr. Ebru Harmandar (Supervisor) Signature:
Muğla Sıtkı Koçman University, Muğla

Date of Defence: 12/08/2021

I declare that the thesis titled “ Seismic resilience of a school building in Milas/Mugla” is my own work and is written following all of the ethical rules under the supervision and guidance of Assist. Prof. Dr. Ebru HARMANDAR. I also declare that the information and materials taken from other sources are referenced originally as it is required by thesis rules.

ZUBAIR SEDIQI

12/08/2021

ACKNOWLEDGEMENTS

Firstly, I am extremely grateful to Assist. Prof. Dr. Ebru HARMANDAR for being my advisor and I would like to thank her for her efforts, guidance, supports and selecting such a favorable topic for my thesis. Her immense knowledge and academic experience helped and motivated me in my academic researches and my daily life.

Besides, I would like to express my gratitude to my friends and colleagues who helped, encouraged and supported me in my academic and daily life.

Finally, I would like to extend my sincere thanks to my parents and all my family members who always supported and belief in me.

ÖZET
MİLAS/MUĞLA'DA BİR OKULUN SİSMİK DİRENÇLİLİĞİ

Zubair SEDIQI

Yüksek Lisans Tezi

Fen Bilimleri Enstitüsü

İnşaat Mühendisliği Anabilim Dalı

Danışman: Dr. Öğr. Üyesi Ebru HARMANDAR

Ağustos 2021, 50 sayfa

Bir yapısal sistemin sismik dirençliliğinin amacı, depremden kaynaklanan hasarları (can kaybı, sosyal, ekonomik, yapısal ve yapısal olmayan hasarlar) önlemek, en aza indirmek veya azaltmaktır. Yapıların sismik direnci, deprem ve yapı mühendisliğinde gelişmekte olan bir konudur. Son yıllarda deprem mühendisliği araştırmacıları ve uzmanları arasında popüler ve en çok tartışılan konulardan biri olmuştur. 'Dirençlilik' kelimesinin anlamı alandan alana farklılık gösterir, ancak deprem ve yapı mühendisliğinde bir yapısal sistemin hasar gördükten sonra işlevselliğine geri dönmesi anlamına gelir. Okullar, toplumu doğrudan etkileyen en önemli özel mühendislik yapılarından biridir. Bu nedenle, bir deprem meydana geldikten sonra okulları mümkün olan en kısa sürede kurtarmak önemlidir. Bu çalışmada, Türkiye deprem tehlike haritasına göre yüksek deprem potansiyeli olan Muğla'nın Menteşe ilçesinde bir okul binasının depreme karşı dirençlilik çalışmasının yapılması hedeflenmiştir. Araştırma çalışması altı adımdan oluşmaktadır: (1) Sismik tehlike analizi, (2) Okul binasının modellenmesi, (3) İtme analizi, (4) Kırılganlık eğrileri, (5) Hassaslık eğrileri, (6) İşlevsellik eğrileri, (7) Sismik dayanıklılık. Hasar tespit metodolojisi HAZUS'a göre yapılmaktadır. Bina, SAP2000 yapı analiz program kullanılarak modellenerek doğrusal olmayan statik itme analizi uygulanmıştır. Bu çalışma, deprem sırasında can kayıplarının, ekonomik kayıplarının ve okul binalarının deprem sonrasında toparlanma sürelerini azaltmaya ve başka okul binalarının dirençlilik hesaplamalarında altlık oluşturacaktır.

Anahtar Kelimeler: Sismik Dirençlilik, Okul Binaları, Hasar Değerlendirmesi, Binaların İşlevselliği, İyileşme Analizi.

ABSTRACT

SEISMIC RESILIENCE OF A SCHOOL BUILDING IN MILAS/MUGLA

Zubair SEDIQI

Master of Science (M.Sc.)
Graduate School of Natural and Applied Sciences
Department of Civil Engineering
Supervisor: Assist. Prof. Dr. Ebru HARMANDAR
August 2021, 50 pages

Aim of the seismic resilience of a structural system is to prevent, minimize or decrease the damages (loss of life, social, economic, structural, and non-structural damages) that occur due to earthquake. Seismic resilience of structures is one of the most interesting topics in the field of earthquake and structural engineering. It has been a popular and one of the most discussed topics for the researchers and specialists of earthquake engineering in the recent years. The meaning of the word 'resilience' differs from field to field, but in earthquake and structural engineering resilience means returning of the functionality of a structural system after it has been damaged. Seismic resilience of structures is a developing topic in earthquake and structural engineering. Schools are one of the most important special engineering structures that directly affect the public. Therefore, it is important to recover schools as soon as possible after occurring of an earthquake. A seismic resilience study for a school building of Milas, Mugla which is one of the most hazardous earthquake areas in Turkey according to the hazard map is performed. The building is studied according to the hazard map and the predefined earthquake scenarios. The research study has six steps as: 1) Seismic hazard analysis, (2) Modeling of the school building, (3) Pushover analysis, (4) Fragility curves, (5) Vulnerability curves, (6) Functionality curves, (7) Seismic resilience. The damage assessment methodology is done based on HAZUS. SAP2000 software is used for modeling and nonlinear static pushover analysis is performed. This study will help and bring improvements in seismic resilience of school buildings and reduce social, economic damages and fatalities during

an earthquake and recovery time of school buildings after an event. It will be a base input for the resilience of other school buildings as well.

Keywords: Seismic Resilience, School Buildings, Damage Assessment, Functionality of Buildings, Recovery Analysis.

TABLE OF CONTENTS

LIST OF TABLES

LIST OF FIGURES

LIST OF SYMBOLS AND ABBREVIATIONS

A_d	Design Acceleration (Capacity Spectrum)
A_u	Ultimate Acceleration (Capacity Spectrum)
A_y	Yield Acceleration (Capacity Spectrum)
CP	Collapse Prevention
C	Collapse
(Cs,j)	Repairing Cost
C1L	Low Rise Reinforced Concrete Building
D_d	Design Displacement (Capacity Spectrum)
D_y	Yield Displacement (Capacity Spectrum)
D_u	Ultimate Displacement (Capacity Spectrum)
D	Displacement
DD-2	10% Probability of Exceeding in 50 Years, Corresponding to a Return Period of 475 Years.
ds	Damage State
EMS98	European Macroseismic Scale
$F_{İE}$	Seismic Load
F_S	Local Soil Effect Coefficients for Short Period
F_1	Local Soil Effect Coefficients for One Second Period
f_{cd}	Design Compressive Strength
f_{ck}	Characteristic Compressive Strength
f_{yd}	Design Yield Strength of Reinforcements
f_{yk}	Characteristic Yield Strength of Steel Reinforcement
G	Dead Load
H	Heaviside Function
IDA	Incremental Dynamic Analysis
IO	Immediate Occupancy
I_S	Replacement Cost
K	Awareness Factor
LS	Life Safety
L	Loss Functionality

L_D	Direct Loss
L_I	Indirect Loss
MDF	Mean Damage Factor
M	Mass of the Structure
M_{ib}	Torsional Moment (due to seismic load with 5% eccentricity)
PGA	Peak Ground Acceleration
P	Probability
Q	Live Load
Q(t)	Functionality of the structure
R	Resilience
RC	Reinforced concrete
r_i	Annual Discount Rate
r_k	Damage Ratio of Each Damage State
S_{DS}	Short Period Design Spectral Acceleration
S_{D1}	Design Spectral Acceleration for One Second
$S_{ae(T)}$	Elastic Spectral Acceleration
S_S	Short period Spectral Acceleration Coefficient
S_1	Spectral Acceleration Coefficient for One Second Period
S_d	Spectral Displacement
$\bar{S}_{d,}ds$	Median Spectral Acceleration of a Damage State
S_{dy}	Yield Spectral Displacement
S_{du}	Ultimate Spectral Displacement
T_{RE}	Recovery Time
T_{LC}	Control time
T_A, T_B	Design Spectrum Corner Periods
T_i	Time Range Between the First Investment and Extreme Event
T_L	Long Period (Transition Period)
t_{0E}	Event Time
$(Vs)_{30}$	Average Seismic Shear Wave Velocity from Surface to 30 meters depth
V	Base Shear
W	Total Self Weight of the Structure

β_{ds}	Standard Deviation of the Natural Logarithm of Damage State
Φ	Standard Normal Cumulative Distribution Function
δ_i	Annual Depreciation Rate
γ_c	Material Coefficient of Concrete
γ_s	Material Coefficient of Steel
κ	kappa factor (degradation factor)

1.INTRODUCTION

Seismic resilience of structures is one of the most interesting topics in the field of earthquake and structural engineering. It has been a popular and one of the most discussed topics for the researchers and specialists of earthquake engineering in the recent years. Meaning of the word resilience differs from field to field, but in earthquake and structural engineering resilience means returning of the functionality of a structural system after it has been damaged (Figure 1.1). Generally, in this topic these two issues, loss of functionality and recovery time of structural system are discussed. In order to evaluate the seismic resilience of a structural system some analyses and assessments such as seismic hazard analyses, damage assessment and functionality curves should be discovered through the procedure. Seismic resilience is important for economical purposes and for safety of people especially in prone-earthquake areas.

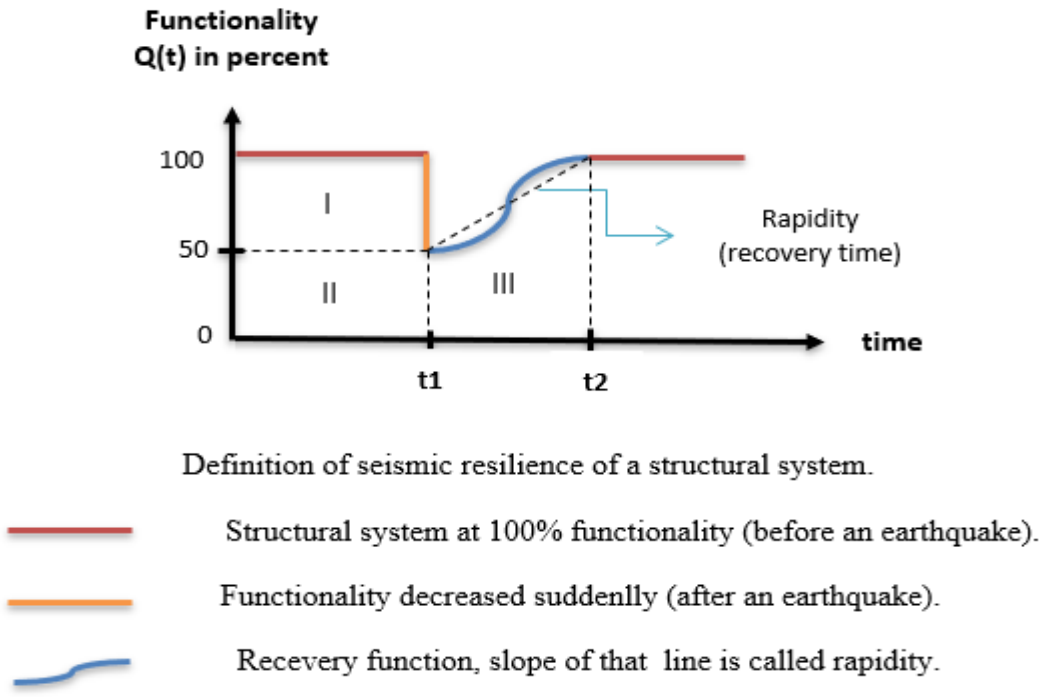

Figure 1.1. Definition of seismic resilience of a structural system (Bruneau, 2003)

Bruneau (2003) derived a mathematical formula for resilience (R) as follow

$$R=\int_{t1}^{t2}[100-Q(t)]dt \quad (1.1)$$

where Q(t) is quality of a structural system as a function of time.

A resilience system should have the following properties (Bruneau, 2003):

- Robustness: the strength or ability of a structure that can withstand against an event without losing functionality of the structural system (the undamaged part of the structure).
- Redundancy: is the availability of substitutional structural elements that can be used instead of the structural elements that are destroyed or lost its functionality due to earthquake.
- Resourcefulness: is the ability to determine risky conditions that put the structure at risk which can cause to damage some structural elements or systems.
- Rapidity: is the time in which the structure can gain its desired functionality again.

As shown in Figure 1.1, the resilience curve is divided into three parts. The first part is called functionality loss, it is part of the structure that can not withstand against an event. Second part of the curve is called robustness which can withstand against the event without losing any functionality. Third part of the curve is the area under recovery function and is called resilience, slope or tangent of the recovery function line is called rapidity which shows how quick the structure will receive its previous functionality.

2.LITERATURE REVIEW

For the first time, the concept of seismic resilience was explained by (Bruneau, 2003) as shown in Figure 1.1. Then, Bruneau (2004) developed an idea about resilience of acute care facilities, this idea has been developed based on two options, quality of life (total health population) and hospital capacity. Furthermore, they studied on the resilience of structural and non-structural elements as well. Researchers have been trying to present a suitable seismic resilience methodology for acute care facilities. Cimellaro (2005) proposed a framework for resilience of hospitals and they applied the methodology to a hospital in California. The methodology takes the important factors of resilience into consideration such as loss function (direct and indirect losses) and fragility curves which are used for damage assessment of structures. A new methodology for seismic resilience of hospitals was developed by Cimellaro (2010) taking into consideration the uncertainties (losses, recovery time, intensity parameters, response parameters) of seismic resilience. The framework methodology was applied on six hospitals in Memphis, USA taking into account several rehabilitation strategies. They concluded that the rebuild strategy show the highest resilience and function of quality. But it is the most uneconomically option.

The methodology for resilience of a single building and group of buildings in a region is not exactly the same. For regional buildings the resilience procedure is applied based on the building inventories which are grouped according to the buildings properties such as geometry, number of story etc. Burton (2017) recommended a framework for the resilience of regional buildings. This study shows repairing ways for each limit states (collapse, demolish, irreparable damages, loss of functionality) of a structure and a non-linear time history analyses is performed for damage assessment and fragility curves. Xiong (2020) derived a methodology for seismic resilience of Beijing city. Non-linear time history analysis and FEMA-P58 methodology is used to get fragility curves and the residually functionality of each building for the post-earthquakes of the region.

Like hospitals, schools are one of the most important civil engineering structures as well. Researchers and engineers have been searching to find an appropriate and safe way for

the resilience of school buildings. In the recent years, some studies about school buildings resiliency have been done. Samadian (2019) conducted a research study for a reinforced concrete (RC) school building based on vulnerability curves. The authors concluded that resilience functionality obtained using vulnerability curves give more actual results than those gained using fragility curves. Motlagh (2020) evaluated a seismic resilience of RC school building taking into consideration the effects of carbonate corrosion. The authors concluded that the corrosion effects negatively the resilience of structures. González (2020) made a research study for the resilience of school buildings in Mexico according to event-based assessment methodology and he derived that one-story buildings are more resilient than two story buildings because the number of casualties in two story buildings are higher due to structural and non-structural damages. Finally, Sardari (2020) analyzed a seismic resilience case study of a high school steel building. The proposed framework was applied to a retrofitted and un-retrofitted school building, the study showed that retrofitted buildings' loss functionality is decreased, but the resiliency is increased.

In this study, the resiliency of a high school building which is located in Milas/Mugla, Turkey is studied. According to General Directorate of Mineral Research and Exploration of Turkey, Mugla is one of the hazardous and earthquake prone areas which has many active faults as shown in Figure 2.1.

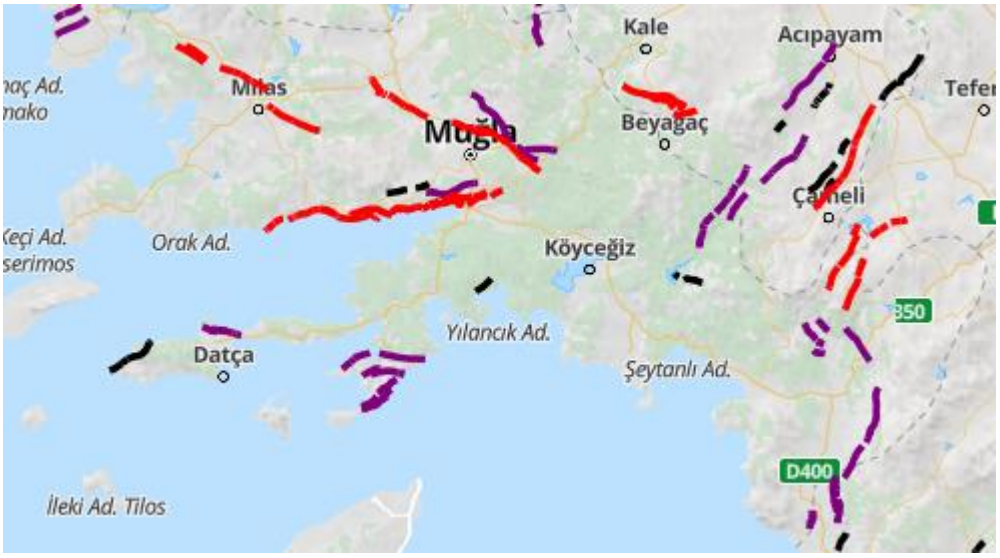

Figure 2.1. Active fault map of Mugla

The main fault zones in this city are, Büyük-Menderes fault zone, Karaove-Milas fault zone, Muğla-Yatağan fault zone, Gökova fault zone, Fethiye-Burdur fault zone. Fault direction in this region is generally from east to west with lateral and strike-slip (İnce, 2021) and normal mechanism. The targeted school is located in the Milas district which has the Karaova-Milas active fault zone. According to İnce (2021), Karaova-Milas fault zone is a combination of parallel faults from NW to SE direction with a length of about 20 km (Figure 2.2.).

Figure 2.2. Karaova-Milas fault zone

As mentioned before, schools are one of the most important special engineering structures that every student should reach. Therefore, it is important to recover schools as soon as possible after occurring of an earthquake. This study will help and bring improvements in seismic resilience of school buildings and can reduce social, economic damages and fatalities. Moreover, it will help engineers and civilians to prevent or decrease number of casualties during an earthquake, enhance seismic resilience of the school buildings, take precautions for the future earthquakes, develop the design of the school buildings in the region for the post-earthquakes, asset the probability of buildings' damages and loss of functionalities. Procedure of this study will cover some important topics such as, seismic hazard analysis, modeling, building capacity, damage assessment (fragility and vulnerability curves) and the functionality curve. All these subjects will be discussed in details in the next parts of this thesis.

3.METHODOLOGY

3.1 Framework of The Study

Summary of the framework for this study is shown in Figure 3.1.

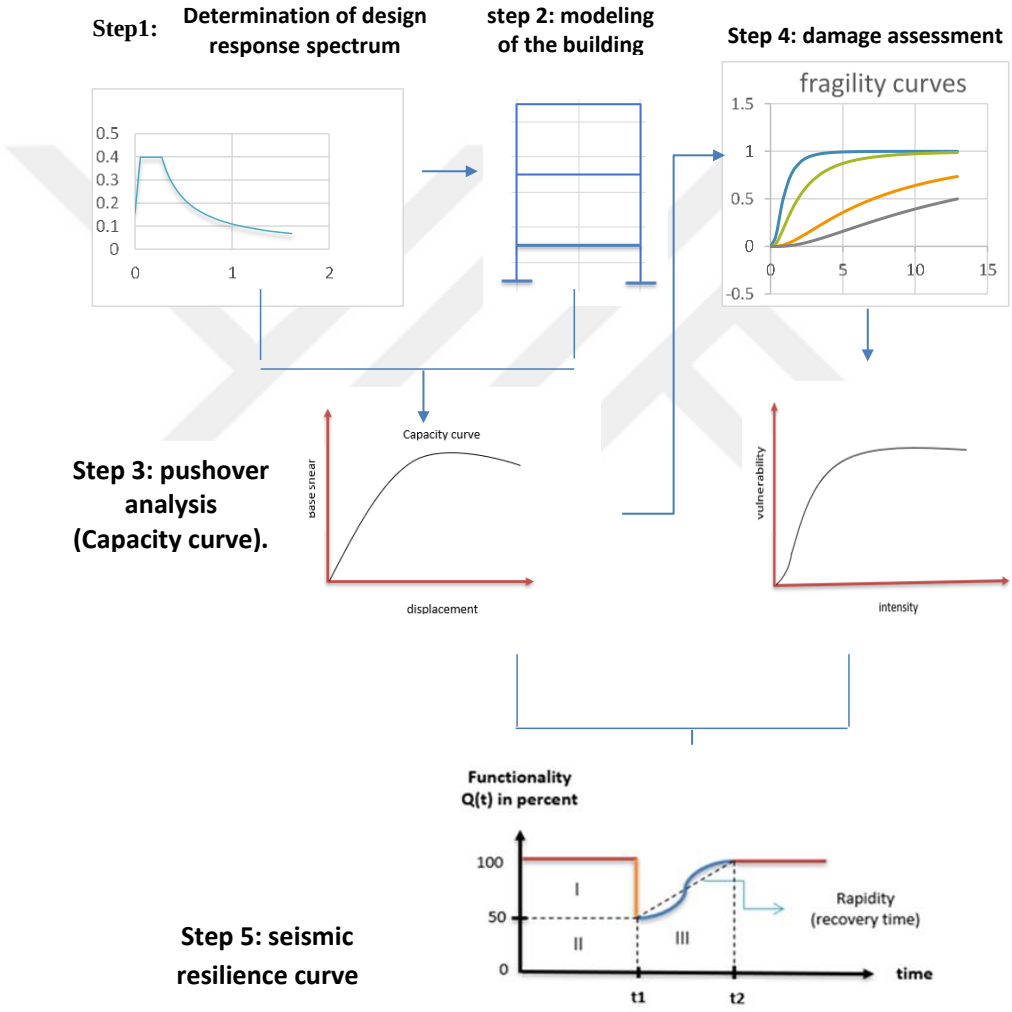

Figure 3.1. Framework of the study (Samadian, 2019)

3.2 Determination of Design Response Spectrum

For seismic hazard analysis, seismic hazard map (Figure 3.2.) which is prepared by Disaster and Emergency Management Presidency (AFAD) is used. By the help of this

map, we can understand that which part of the country has the high potential earthquakes.

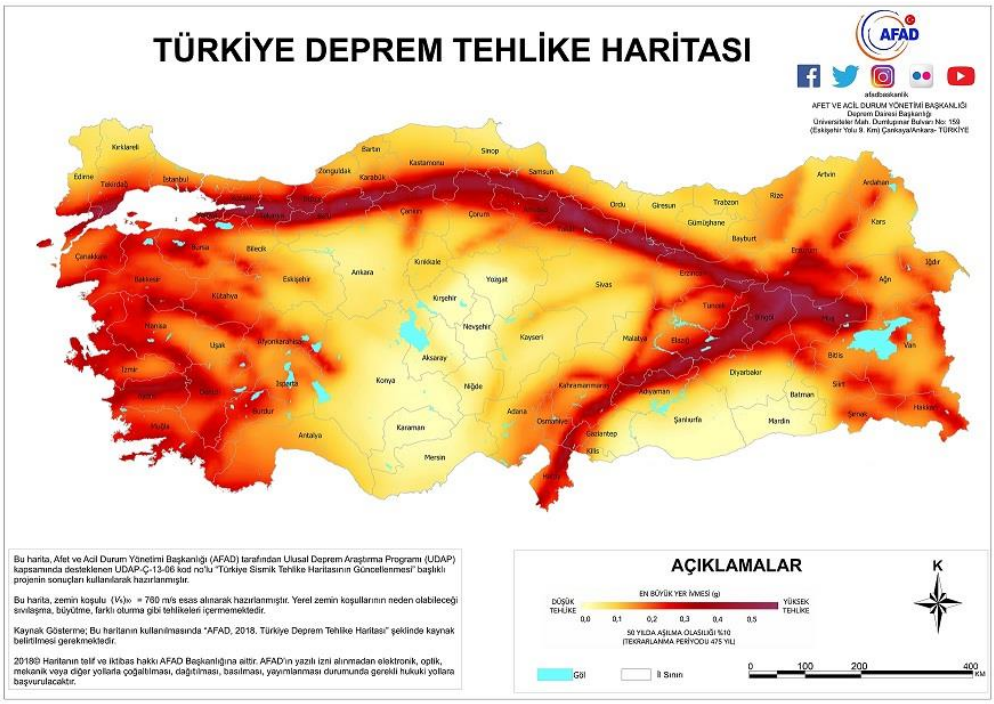

Figure 3.2. Seismic hazard map of Turkey (AFAD)

According to AFAD seismic hazard map the required parameters for response spectrum are obtained. Then by using equation (3.1) which is prepared by Turkish Building Earthquake Code (TBEC, 2018), the response spectrum (Figure 3.3.) of a specific region is determined.

$$
\begin{aligned}
S_{ae}(T) &= \left(0.4 + 0.6\frac{T}{T_A}\right)S_{DS} && (0 \le T \le T_A)\\
S_{ae}(T) &= S_{DS} && (T_A \le T \le T_B)\\
S_{ae}(T) &= \frac{S_{D1}}{T} && (T_B \le T \le T_L)\\
S_{ae}(T) &= \frac{S_{D1}\,T_L}{T^2} && (T_L \le T)
\end{aligned}
\qquad (3.1)
$$

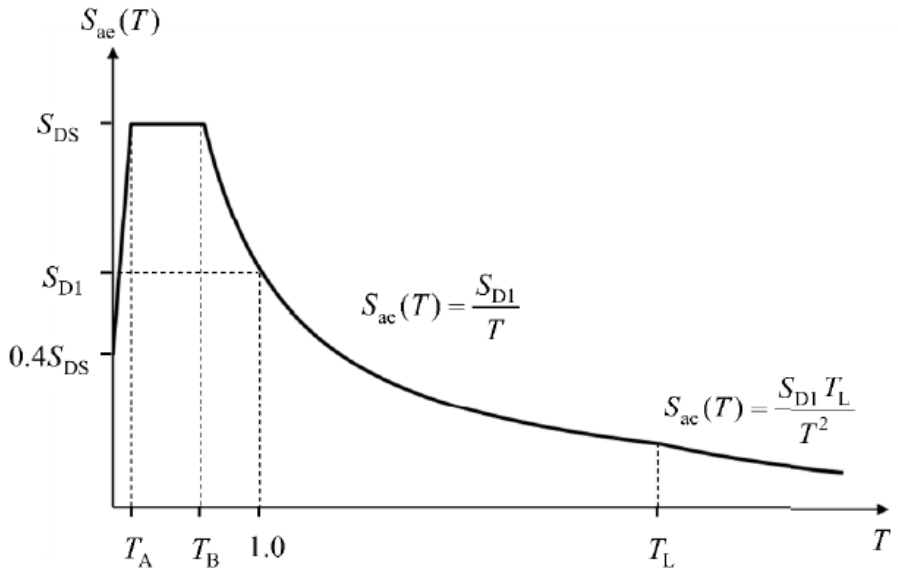

Figure 3.3. Design response spectrum (TBEC, 2018)

The parameters of design response spectrum are calculated by the following equations:

$$S_{DS}= S_S F_S \qquad S_{D1}=S_1 F_1 \qquad T_A=0.2\,(S_{D1}/S_{DS}) \qquad T_B=S_{D1}/S_{DS} \tag{3.2}$$

The values of F_S and F_1 can be taken from the table (Table 3.1.) which is prepared by the TBEC (2018) based on the soil class and the values of S_S and S_1.

Table 3.1. Local soil effect coefficients for F_S and F_1 (TBEC, 2018)

Local Soil Class	**Local soil effect coefficients for short period (F_S)**					
	$S_S \leq 0.25$	$S_S=0.5$	$S_S=0.75$	$S_S=1$	$S_S=1.25$	$S_S \geq 1.5$
ZA	0.8	0.8	0.8	0.8	0.8	0.8
ZB	0.9	0.9	0.9	0.9	0.9	0.9
ZC	1.3	1.3	1.2	1.2	1.2	1.2
ZD	1.6	1.4	1.2	1.1	1.0	1.0
ZE	2.4	1.7	1.3	1.1	0.9	0.8
ZF	Site-specific soil behavior analysis will be performed					

Table 3.2. Local soil effect coefficients for F_S and F_1 (TBEC, 2018) (continued)

Local Soil Class	Local soil effect coefficients for one second period (F_1)					
	$S_1 \leq 0.1$	$S_1=0.2$	$S_1=0.3$	$S_1=0.4$	$S_1=0.5$	$S_1 \geq 0.6$
ZA	0.8	0.8	0.8	0.8	0.8	0.8
ZB	0.8	0.8	0.8	0.8	0.8	0.8
ZC	1.5	1.5	1.5	1.5	1.5	1.4
ZD	2.4	2.2	2.0	1.9	1.8	1.7
ZE	4.2	3.3	2.8	2.4	2.2	2.0
ZF	Site-specific soil behavior analysis will be performed					

3.3 Performance Analysis of a Structure

3.3.1 Seismic Capacity

For the dynamic analysis of the structures and as a result to obtain capacity curve of the structure, it is required to do a nonlinear static pushover or incremental dynamic analysis of the building. For modeling and non-linear analysis of the structure several structural software can be used. In this study, SAP2000 software is used to model and analyze the structure. The structure is modeled according to Turkish Building Earthquake Code (TBEC, 2018) and TS-498. Pushover analysis method is one of the dynamic analysis methods which is used widely for seismic performance of buildings. Therefore, in this study seismic performance of the structure is analyzed based on the non-linear static pushover analysis. Capacity curve (pushover curve) of a structure is obtained as roof-displacement and base shear of the building under monotonic lateral loads and the self-weight (dead load) of the structure (Figure 3.4.).

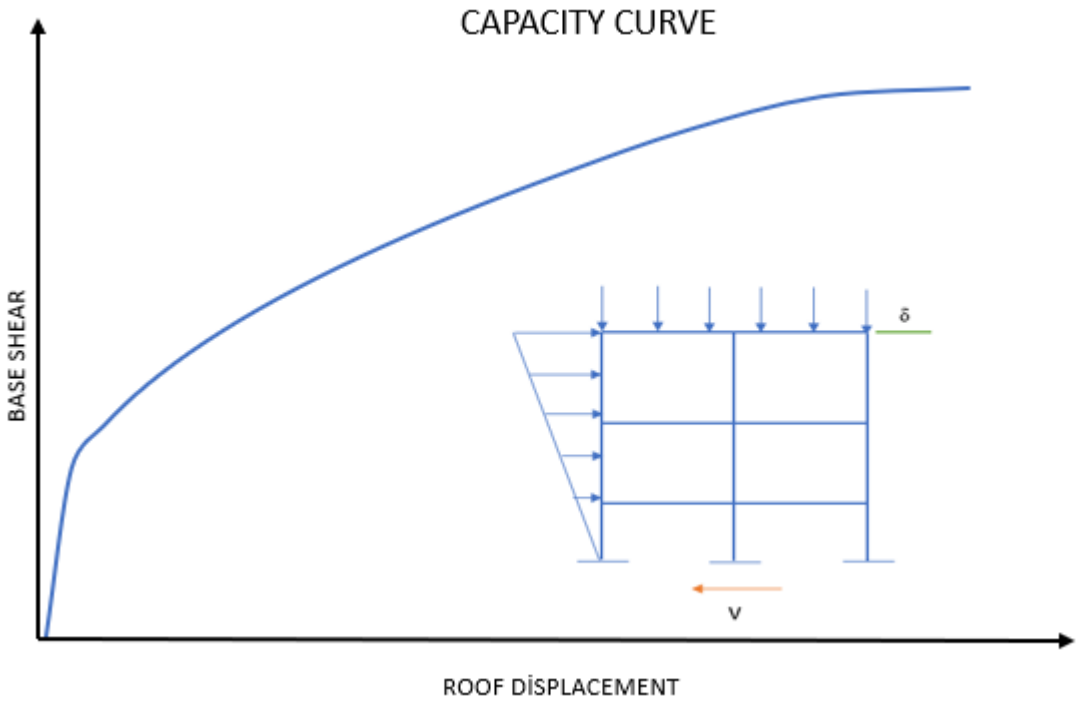

Figure 3.4. Capacity curve of a structure and its required loads

A capacity curve is a combination of three control points (Figure 3.5.) which are called:

- Design capacity
- Yield capacity
- Ultimate capacity

Where design capacity exemplifies the nominal strength of a building, yield capacity shows the real strength of a building. Last control point describes the maximum strength which a building can withstand and after that the structure lose it elasticity and reach the plastic stage (HAZUS-MH-MR4).

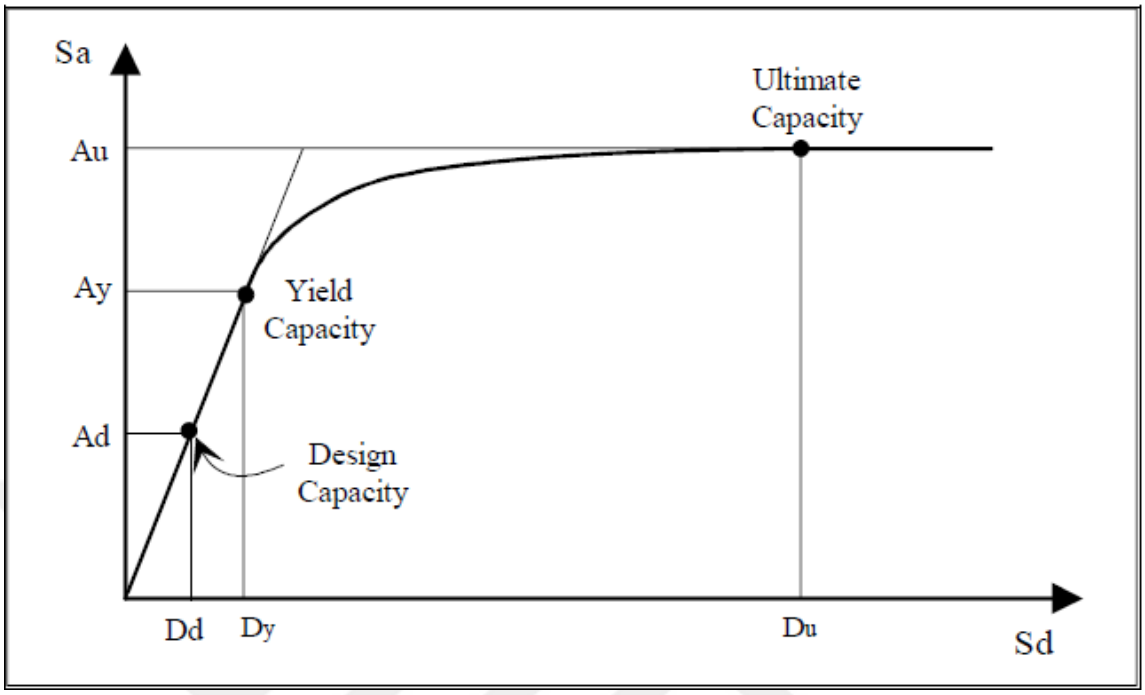

Figure 3.5. Control points of a building capacity curve (HAZUS-MH-MR4)

3.3.2 Performance Levels and Seismic Damage

Another important issue in the analyses is assigning the plastic hinges to beams and columns. M3 and P-M2-M3 hinges are assigned to both ends of beam and columns respectively and the whole structure is assumed to be diaphragm in the vertical global (Z) direction. The plastic hinges have several performance levels (plastic hinge deformations) as shown in Figure 3.6. Based on these plastic hinge deformations, we can estimate the probable damages that will occur in the structure during a natural hazard. The damage level increase gradually from (A-C), at point (C) the structure fails, lose its functionality suddenly and as a result it will collapse. Every performance level has a specific damage definition. Hamadamin (2014) defined some of the performance levels as follows:

- (A-B) performance level: very small damages can occur that can be ignored or requires very small repairs.
- (B-IO) performance level: limited or very slight structural damages can occur, but the systems and building structure can be rationally applicable.

- (IO-LS) performance level: due to structural and non-structural damages a low life safety threatening is expected.
- (LS-CP) performance level: there is a possibility of collapsing and the frame of the building will see structural damages, because of that the structure may not withstand against lateral forces and can support only gravity loads.

For better understanding Figure 3.7 shows the damage and performance levels of a structure with more details.

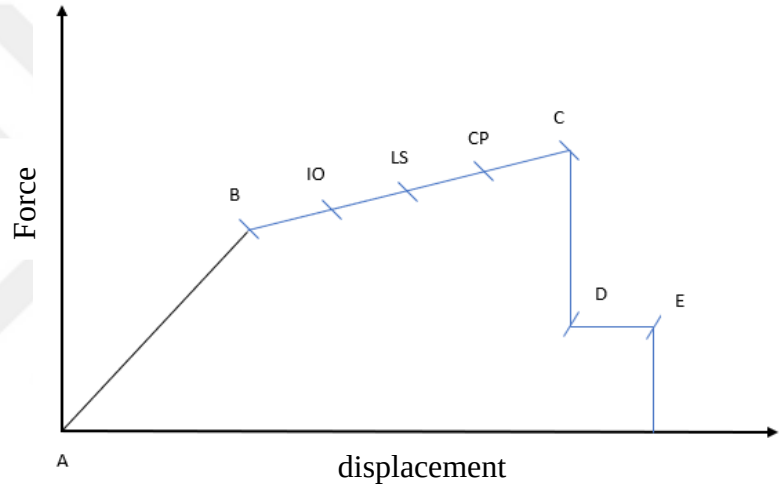

Figure 3.6. Performance levels of plastic hinges

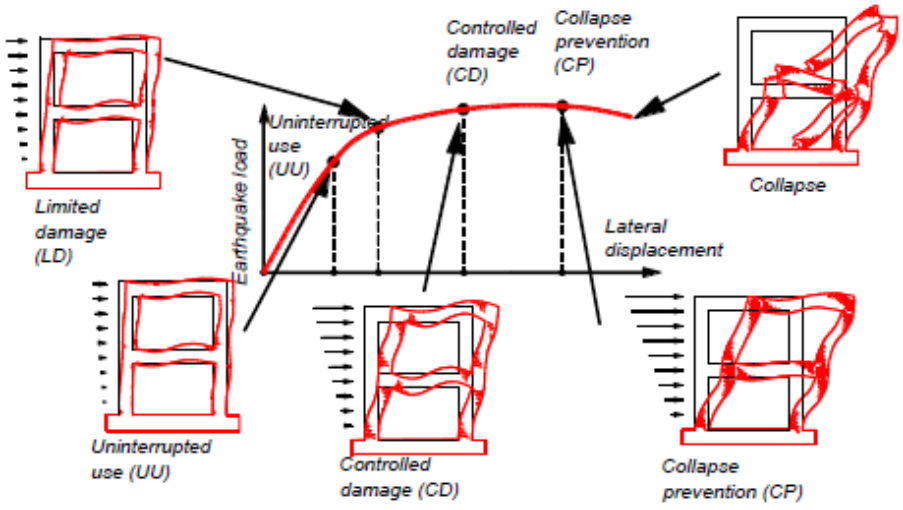

Figure 3.7. Performance levels of a building (Güler, 2020)

3.4 Damage Assessment (Seismic risk assessment)

Damage assessment of structures can be divided into two main parts:

- Fragility analysis
- Vulnerability analysis

3.4.1 Fragility analysis

Fragility analysis (Fragility curves) is one of the popular ways for prediction of loss estimation. It describes the damage probability of exceedance of a structure for post-earthquakes. Cimellaro (2006) divided fragility curves into two parts, empirical and analytical fragility curves. Empirical fragility curves are obtained based on the field data which is collected according to the damages occurred to the structures due the past earthquakes. On the other hand, analytical fragility curves can be generated using seismic response data which is obtained from ground motions while analyzing the structure. To obtain the seismic response data, we can use several methods such as, nonlinear time history analysis, nonlinear static analysis, and elastic spectra analysis. Fragility curve (Figure 3.8.) is a plot of earthquake intensity (which can be in terms of spectral displacement (Sd), peak ground acceleration (PGA)) and the probability of exceedance.

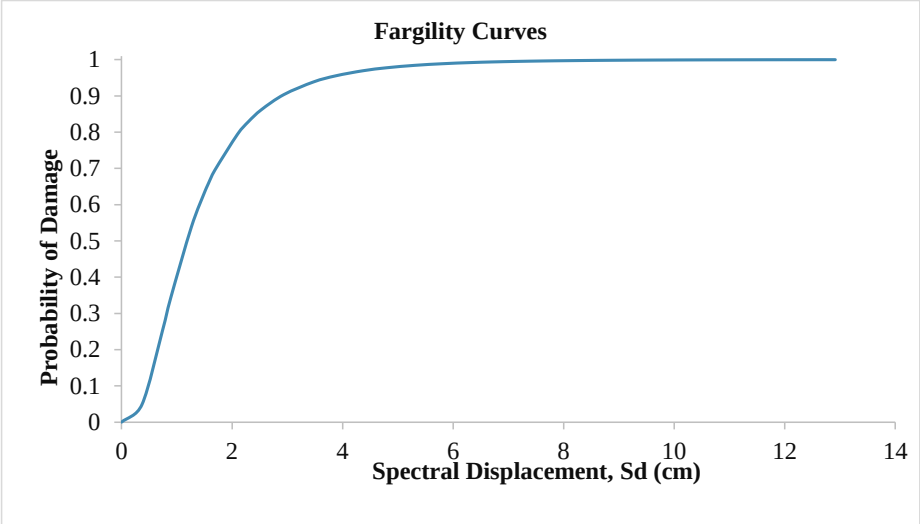

Figure 3.8. Representation of a fragility curve

There are several ways to calculate fragility curves of a structure, HAZUS-MH-MR4 suggested the equation (3.3) for deriving fragility curves.

$$P[(ds|S_d)] = \Phi\left[\frac{1}{\beta_{ds}}\ln(\frac{S_d}{\bar{S}_{d,}ds})\right] \quad (3.3)$$

where:
ds describes the damage state level of a building which can be slight (ds1), moderate (ds2), extensive (ds3), and complete (ds4) damage state.

S_d is the spectral displacement.

$\bar{S}_{d,}ds$ is median value of the spectral displacement for related damage level (ds1, ds2, ds3, ds4).

β_{ds} is standard deviation of the natural logarithm of damage state (ds) and

Φ is the standard normal cumulative distribution function.

Every damage level is described by ($\bar{S}_{d,}ds$) and (β_{ds}) which have different values for each damage level. The (β_{ds}) values can be taken directly from the tables or the formulas which are prepared by HAZUS and the ($\bar{S}_{d,}ds$) values can be achieved by several formulas which are proposed by researchers (Giovinazzi, 2005; Barbat, 2006; Kappos, 2006) and will be discussed with more details in next pages.

3.4.2 Damage levels

According to EMS98 damage levels are described as follows:

- Slight damage level (grade 1): Structural damages are zero or negligible, but a slight nonstructural damage can occur. Very small cracks on the surface of infill and inside (partition) walls can be seen.
- Moderate damage level (grade 2): Small structural damages will occur. But the nonstructural damages are relatively higher than the structural damages. Cracks in beam, column and wall can be seen and plaster in some walls can be fallen.

- Extreme damage level (grade 3,4): This damage level can be divided into two parts, heavy damage level and very heavy damage level. In heavy damage level, moderate structural and massive nonstructural damages occur. Cracks in the critical parts of the structure such as, beam-column joints can be seen. Moreover, breaking of concrete cover, deformation of reinforcements and large cracks in infill and partition walls can be seen. In very heavy damage level (Figure 3.9.), extreme structural damages occur, rebars rupture and there is possibility of compressional failing of structural elements. In addition to this, collapsing of small number of columns is possible as well.

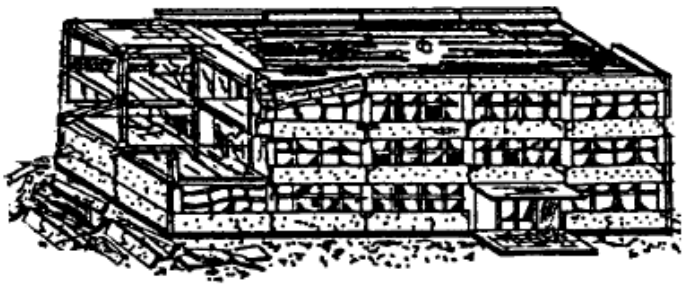

Figure 3.9. Very heavy damage level (EMS-98)

- Destruction (collapse) damage level (grade 5): The whole structure or the main parts of it will collapse completely (Figure 3.10.).

Figure 3.10. Collapse damage level of a structure (EMS-98)

3.4.3 Vulnerability analysis

Vulnerability curve which is a cumulative combination of discrete damage probabilities and mean damage factors (MDFs), shows us damage probability of a structure. Therefore, fragility analysis is a pre-request for the determination of the vulnerability curves.

Vulnerability curves are obtained by Equation (3.4):

$$\text{Vulnerability (\%)} = \sum_{ds=1}^{n}\{\mathrm{P}[\mathrm{ds} = \mathrm{DS}] \times \mathrm{MDF}_{\mathrm{ds}}\} \quad (3.4)$$

where (ds) is damage state, $P[ds = DS]$ is discrete probability of damage state and (MDF_{ds}) is the mean damage factor of a specific damage state (slight, moderate, extensive, collapse).

The MDFs values can be obtained from HAZUS, FEMA-356, ATC-13 and EMS98. In this study, HAZUS methodology is used for the determination of the fragility curves. Thus, the MDFs values prepared by HAZUS (Table 3.2.) are used in this study.

Table 3.3. Mean damage factors according to HAZUS

Damage state	Damage factor range (%)	Mean damage factor (%)
Slight	>0-4	2
Moderate	4-16	10
Extensive	16-84	50
Collapse (complete)	100	100

As shown in Table 3.2, MDF is the average value of the damage factor range.

The HAZUS discrete damage probabilities are obtained using Equation (3.5) to Equation (3.8):

$$\text{P [ds=complete]} = \text{P [ds} \geq \text{complete]} \quad (3.5)$$

$$\text{P [ds=extensive]} = \text{P [ds} \geq \text{extensive]} - \text{P [ds} \geq \text{complete]} \quad (3.6)$$

$$\text{P [ds=moderate]} = \text{P [ds} \geq \text{moderate]} - \text{P [ds} \geq \text{extensive]} \quad (3.7)$$

$$\text{P [ds=slight]} = \text{P [ds} \geq \text{slight]} - \text{P [ds} \geq \text{moderate]} \quad (3.8)$$

Finally, the vulnerability curves (Figure 3.11.) can be generated using equation (3.4).

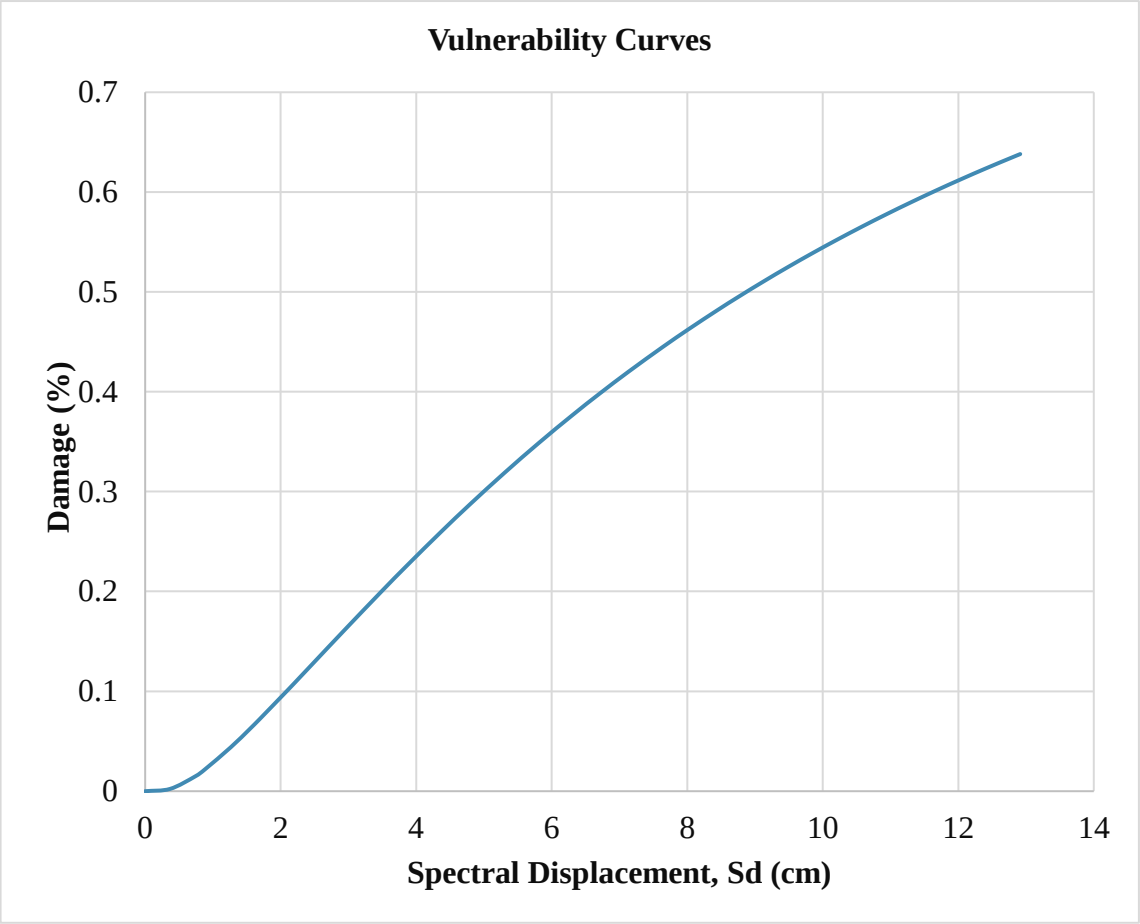

Figure 3.11. Vulnerability curve of a structure

3.5 Seismic Resilience

Last part of the methodology is determination of loss functionality and the seismic resilience of the structure. As shown in Figure1.1, a resilience curve can be divided into three parts. The structure shows 100% functionality until t1, later at t1 when an event occurs a sudden drop in the curve is seen, that sudden decrease is called functionality loss. Second part of the curve which could stand against the event is called robustness. It is the strongest part of the structure which could conserve its functionality against the natural hazard event. Third part of the structure is recovery function. It can be linear,

exponential, or trigonometric (Figure 3.12.). Recovery curve is function of event time. Thus, increase in recovery time (T_{RE}) causes decrease in rapidity and vice versa.

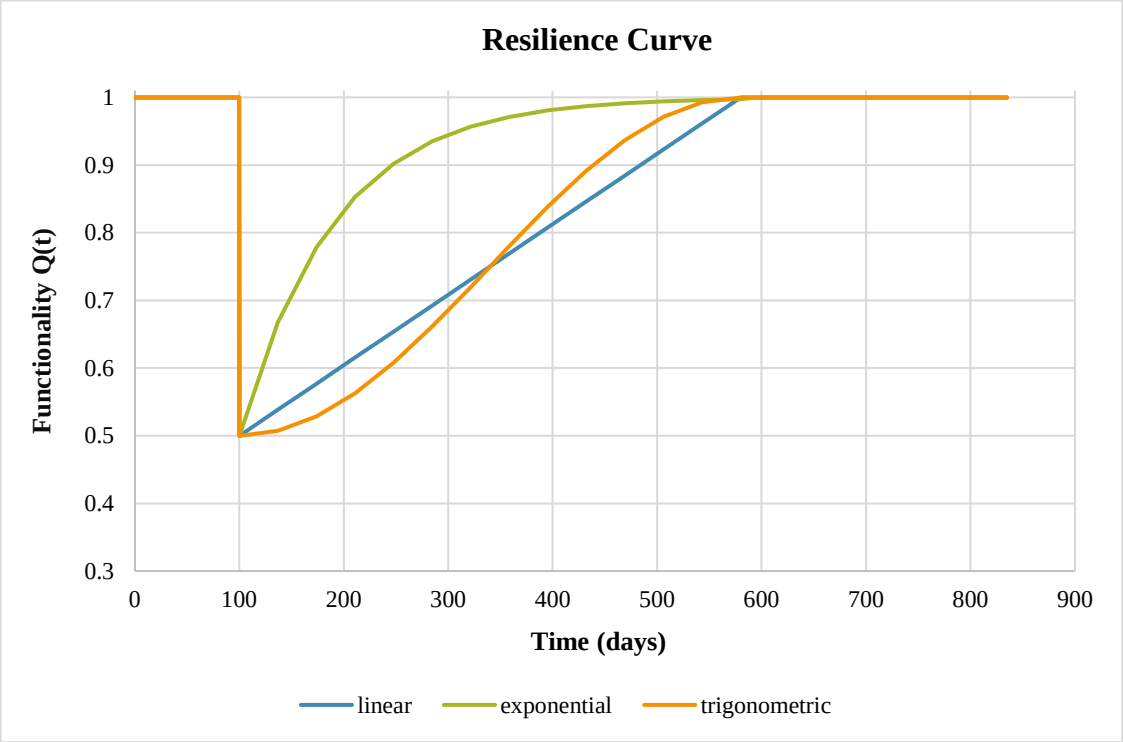

Figure 3.12. Types of recovery curves

3.5.1 The Functionality of a structure

As aforementioned, when a structure is subjected to a hazard event, it loses its functionality. To find the functionality of a structure, equation (3.9) is used:

$$Q(t) = 1 - L(I, T_{RE})\left[H(t - t_{0E}) - H\left(t - (t_{0E} + T_{RE})\right)\right] f_{rec}\,(t, t_{0E}, T_{RE}) \qquad (3.9)$$

where Q(t) is the functionality of a structure, $L(I, T_{RE})$ is the loss functionality, $H(t - t_{0E})$ is the Heaviside function.

As seen from equation (3.9), the functionality function is a combination of three functions such as loss function, Heaviside function and recovery function.

Functionality loss which is dependent on intensity and recovery time can be obtained by several formulas which are derived by researchers, (Ghosh 2021, Samadian 2019) it will be explained in details in the next pages.

Heaviside function is always equal to zero or one which is dependent on the sign of a number. For positive numbers, it takes value of one, for negative numbers it takes value of zero. Shortly, we can write that: $H(\text{positive number or zero}) = 1$, H (negative number) =0.

Recovery function has three types as shown in Figure 3.12. Each of this curve is obtained by a specific equation.

The linear recovery function is obtained by equation (3.10):

$$f_{rec}\,(t, T_{RE}) = (1 - \frac{t - t_{0E}}{T_{RE}}) \tag{3.10}$$

For exponential recovery function:

$$f_{rec}(t) = \exp\,[-(t - t_{0E})(\frac{\text{Ln}\,(200)}{T_{RE}}] \tag{3.11}$$

For trigonometric recovery function:

$$f_{rec}(t) = 0.5\,\{1 + \cos\left[\frac{\pi\,(t - t_{0E})}{T_{RE}}\right]\} \tag{3.12}$$

Linear recovery function is the simplest form which is used when there is lack of details about readiness, accessibility to the sources and social reaction. The exponential recovery function is used when the primary social facilities are available for using, as seen from its curve in Figure 3.12. The rapidity at first days is in a high level, however when it is getting closer to the end the rapidity is getting slower. The trigonometric recovery function is used when there is inadequacy of resources or organizations. The rapidity can be decreased or increased during the repairing procedure (Cimellaro, 2010).

The event time (t_{0E}) is the time in which the event occurs, and it is the time where the structure starts losing its functionality. T_{RE} is the recovery time in which the structure

will be repaired to recover its functionality to the previous form. It is one of the critical issues and can be problematic to choose the correct and exact recovery time. Usually, it is smaller than control time, and the dimension is dependent on seismic intensity and on accessibility to resources materials and employers (Cimellaro, 2010). The control time (T_{LC}) is the economic life of a structure that can be used, usually it is taken 50 years for reinforced concrete structures.

3.5.2 Functionality loss

Earthquake can cause to structural and nonstructural damages. These damages can effect the functionality of a structure, especially structural damages which are directly linked to the functionality loss of a structure. Seismic losses in a structure can be separated into two parts, direct losses (LD) and indirect losses (LI). Direct losses can be in terms of economic and casualties, and indirect losses can be divided into two parts as well. They can be indirect economic losses and indirect casualties (Cimellaro, 2010).

Several formula have been derived for obtaining loss functionality, Cimellaro (2010b) suggested equation (3.13):

$$L_{DE}(I) = \sum_{J=1}^{N}\left[\frac{C_{S,J}}{I_S} \cdot \prod_{i=1}^{T_i}\frac{(1+\delta_i)}{(1+r_i)}\right] \cdot P_J\{\cup_{i=1}^{n}(R_i \geq r_{lim\,i})/I\} \quad (3.13)$$

where (δ_i) and (r_i) are the annual depreciation and discount rates respectively, these two parameters may vary from country to country and even from time to time, for example the depreciation rate in Turkey for reinforced concrete buildings is taken 2%. (Pj) is probability of exceedence, (Ti) is time range between the first investment and occurrence of an extreme event, ($C_{S,J}$) and (I_S) are the repairing and replacement costs of the damaged structure, respectively.

Later, Samadian (2019) proposed equation (3.14):

$$L_{DE}(I) = \frac{1}{K} \cdot \sum_{J=1}^{N}\left[\frac{C_{S,J}}{I_S} \cdot \prod_{i=1}^{T_i}\frac{(1+\delta_i)}{(1+r_i)}\right] \cdot \text{Damage (\%)} \quad (3.14)$$

where, (K) is the awareness factor which indicates quantity of information about a construction quality and is equal to one for structures with full awareness and 0.75 for other cases. Damage (%) value will be determined using vulnerability curves.

Ghosh (2021) developed an equation based on the HAZUS methodology taking into consideration only the structural damages. The equation is described as:

$$L_D = \sum P_E\,(DS = K) \times r_k \quad (3.15)$$

where $P_E\,(DS = K)$ is discrete damage probability, (r_k) is the damage ratio of each damage state and has a specific value for every damage state which is prepared by HAZUS. The values prepared by HAZUS are shown in Table 3.3.

Table 3. 4 HAZUS damage ratios (r_k) for buildings

Damage state (ds)	Damage ratio (r_k)
Slight	0.10
Moderate	0.40
Extreme	0.80
Collapse	1.00

As seen from Table 3.3, increase in damage grade causes increase in the damage ratio as well. In slight damage state, functionality loss is low but in collapse damage state the functionality loss is very high even it can be lost totally.

4. CASE STUDY: A SCHOOL BUILDING IN MUGLA

4.1 Introduction

Milas is one of the districts of Mugla which is located on 37.3116° N, 27.7808° E coordinates. As shown in Figure 2.2, it is an active fault zone which is called Karaova-Milas fault zone. A brief information about the seismicity of Mugla city was given in Section 2. In this case study, a school building which has four stories (basement + three normal floors) and is constructed in (576 m^2) area, will be discussed. Dimensions of the building are shown in (Table 4.1.).

Table 4.1. Story heights and dimensions of structural elements

No	Part of structure	Dimension
1	Basement story height (m)	2.9
2	Normal story height (m)	2.8
3	Beam (cm)	30×40
4	Foundation columns (cm)	40×40
5	Normal floor columns (cm)	35×35
6	Slab thickness (cm)	15
7	Shear wall thickness (cm)	25
8	Building width (m)	16
9	Building length (m)	36

Based on the soil mechanics laboratory tests' results, the soil class is selected ZB. According to TBEC (2018), ZB is a group of soil which has slightly weathered, medium tough rocks and has $(Vs)_{30}$ of (760-1500) m/s. Soil class is one of the important parameters for defining of design response spectrum parameters such as, S_{DS} and S_{D1}.

As shown in the 3D-view of the structure (Figure 4.1.), basement floor of the building has shear walls, and the structure has a very small irregularity only to one direction (y-direction), it is due to the shear walls of the stairs (Figure 4.2.) which cause to a small eccentricity on the y-direction. Therefore, it is assumed as a regular structure.

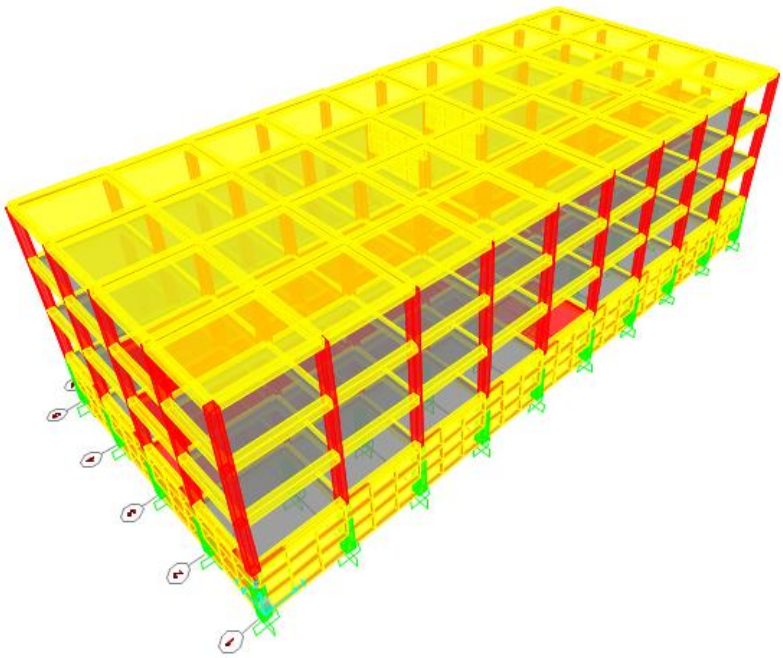

Figure 4.1. 3D-view of the structure

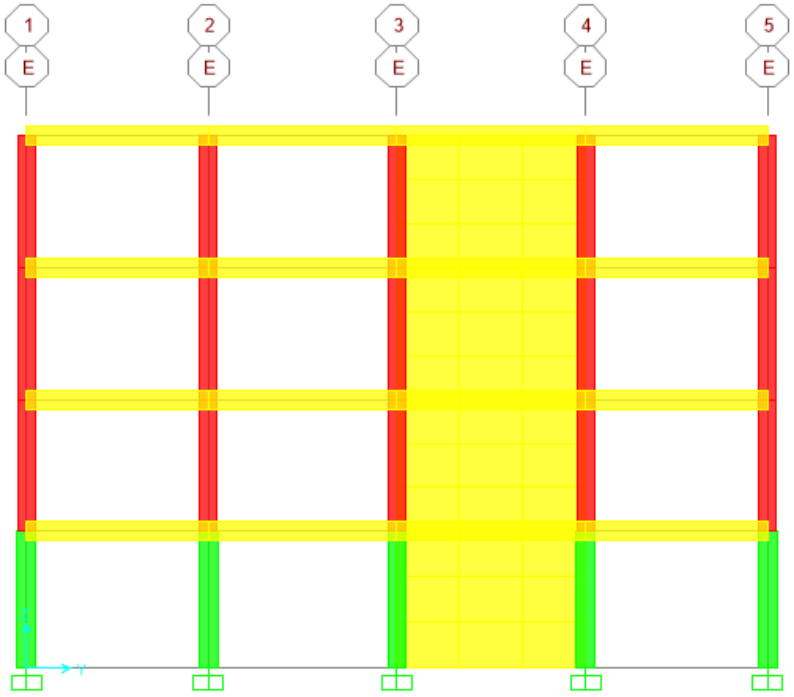

Figure 4.2. Shear-walls of stairs which cause to a small eccentricity to y-direction

Materials used in construction of the building and their properties are shown in Table 4.2.

Table 4.2. Mechanical properties of concrete and steel materials

Material name and its properties		**Material name and its properties**	
C30	Values	S420	Values
f_{ck} (MPa)	30	f_{yk} (MPa)	420
γ_c	1.5	γ_s	1.15
f_{cd} (MPa)	20	f_{yd} (MPa)	365

(f_{cd}) is design compressive strength of concrete which is obtained by dividing the characteristic compressive strength (f_{ck}) on the material coefficient of concrete (γ_c), and (f_{yd}) is design yield strength of reinforcement which is obtained by dividing the characteristic yield strength of steel reinforcement (fy_k) on the material coefficient of steel (γ_s).

4.2 Design Response Spectrum

As shown in Figure 2.2, Mugla has a high possibility of occurrence a strong earthquake. According to the report taken from AFAD based on DD-2 and ZB soil class, the values of S_S and S_1 are 0.888 and 0.208 respectively. The other parameters of design response spectrum such as, S_{DS}, S_{D1}, T_A and T_B can be obtained using Table 3.1 based on the aforementioned methodology. The calculated values for design spectrum are shown in Table 4.3.

Table 4.3. Parameters of design response spectrum

S_S	S_1	F_S	F_1	S_{DS}	S_{D1}	T_A (s)	T_B (s)	T_L (s)
0.888	0.208	0.9	0.8	0.7992	0.1664	0.0416	0.208	6

The design spectrum is determined by using the values listed in Table 4.3 and shown in Figure 4.3.

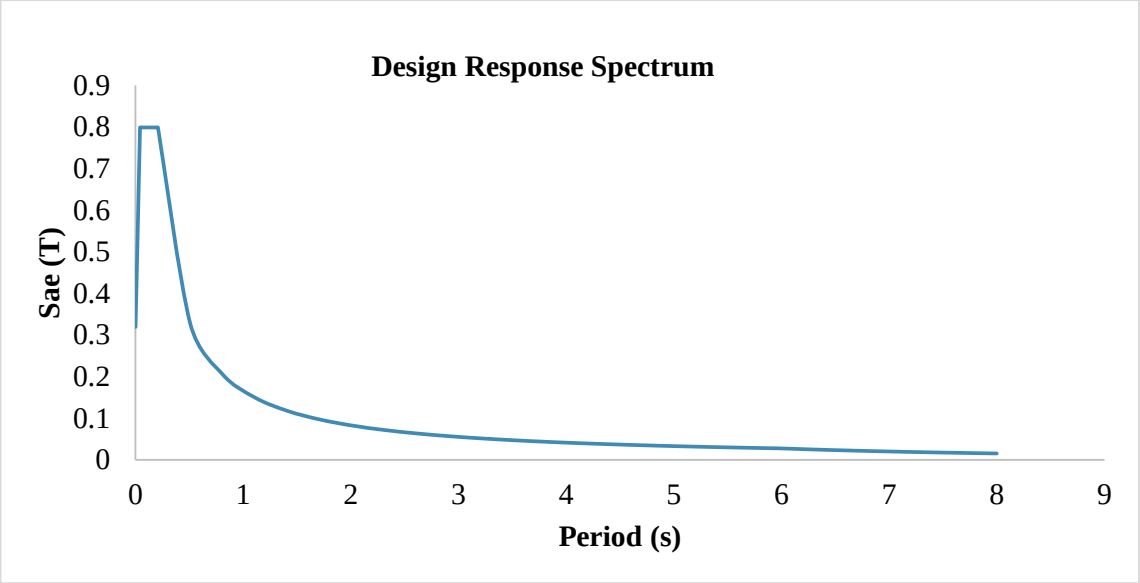

Figure 4.3. Design response spectrum

As shown in Figure 4.3, the design spectrum curve has four different parts: the first part which is started from ($0.4S_{DS}$) and is increased linearly until (S_{DS}) value, second part of the curve which has a constant value of (S_{DS}) and is a straight line which take place between (T_A) and (T_B), third part of the curve is started from (S_{DS}) and the spectral acceleration values are decreasing nonlinearly toward zero until (T_L) value, after (T_L) the fourth part starts and the curve values gets very closer to zero step by step.

4.3 Structural Modeling

Before starting to modeling of the structure, it is necessary to define the loads. The dead and live loads are defined according to TS-498 and seismic loads are calculated based on TBEC (2018). Dead and live loads are shown in Table 4.4.

Table 4.4. Dead and live loads of the structure

Element name	Dead loads (kN/m^2)	Live loads (kN/m^2)
Roof	5	1.5
Normal floor	5.83	3.5
Corridor	5.83	5

After definition of design spectrum parameters and loads, the structure is modeled. The engineering structural software, SAP2000 is used for the modeling of the structure. Figure 4.1 shows the undeformed shape of the modeled building and details of the first five possible deformed mode shapes due to earthquake are shown in Table 4.5.

Table 4.5. Time and frequency of deformed shapes

Mode No	Period (s)	Frequency (Hz)
1	0.62	1.61
2	0.57	1.75
3	0.36	2.77
4	0.2	4.99
5	0.18	5.57

The first mode (Figure 4.4) shows its deformation in x-direction, second mode (Figure 4.5.) is a torsional deformation in z-direction which cause displacements in (x) and (y) directions. Third possible deformation (Figure 4.6.) is displacement of the structure in y-direction.

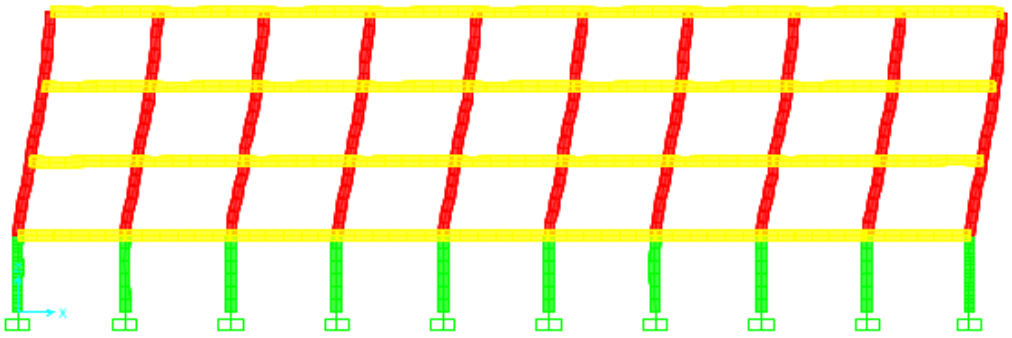

Figure 4.4. Mode-1 of the structure

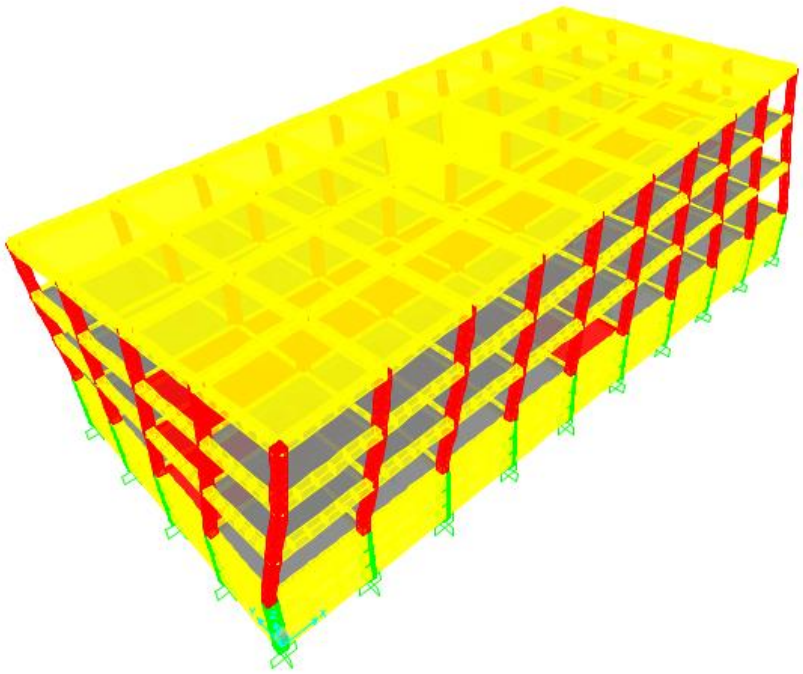

Figure 4.5. Mode-2 of the structure

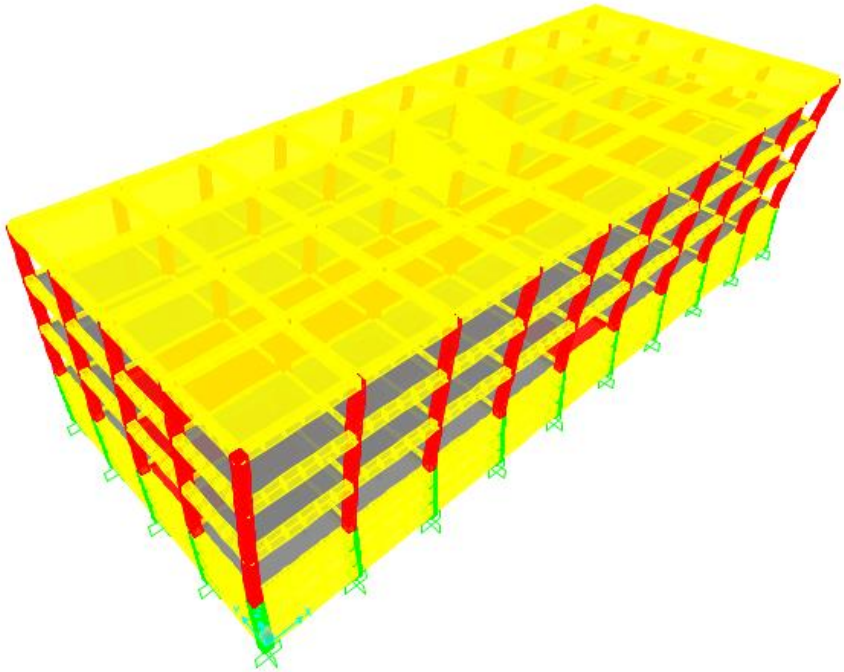

Figure 4.6. Mode-3 of the structure

4.4 Pushover Analysis

Nonlinear static pushover analysis is one of the most commonly used methods for seismic analysis of buildings. In order to perform pushover analysis, it is necessary to obtain seismic loads acting on the building. The total self-weight of the structure is calculated using equation (4.1):

$$W=G+nQ \quad (4.1)$$

where G is dead load, Q is live load and n is load factor which is taken as 0.6 in this study. Thus, total weight is summation of the dead load and sixty percent of the live load. The calculated seismic loads are shown in Table 4.6.

Table 4.6. Seismic Loads of the Structure

Floor No	G (kN)	Q (kN)	W (kN)	M (t)	$F_{iE}^{(X)}$ (kN)	$M_{ib}^{(X)}$ (kNm)	$F_{iE}^{(Y)}$ (kN)	$M_{ib}^{(Y)}$ (kNm)
3	8527.88	845.445	9035.075	921	1020.73	834	1108.8	2071.7
2	5709.65	2140.7	6994.08	712.95	526.77	413.5	572.2	1027.18
1	5709.6	2164.7	7008.5	714.42	263.92	207.18	286.71	514.6

The seismic loads are applied to the center of the structure (mass center) to x-direction (Figure 4.7.) with its positive and negative moments, similarly the seismic loads to y-direction with clockwise and counterclockwise moments are applied to the structure.

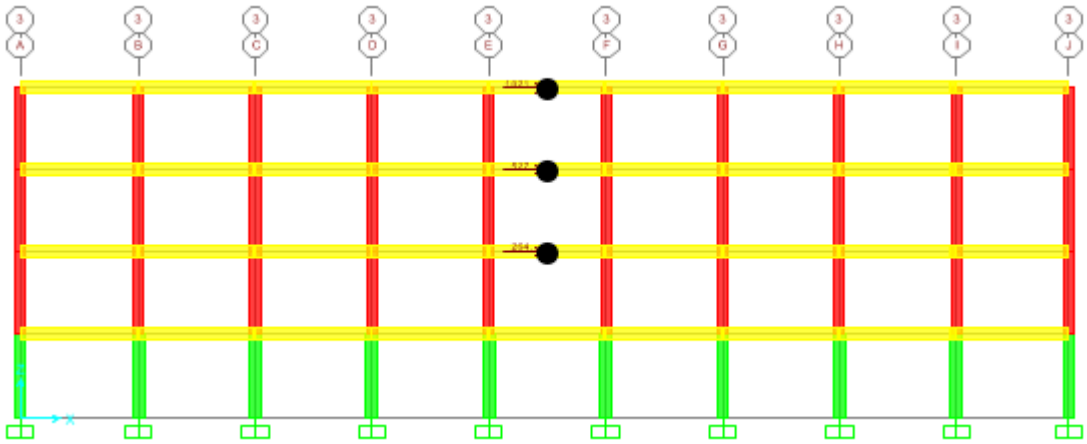

Figure 4.7. Applied fictive loads in x-direction

4.5 Building Response

The structure is analyzed for both (x) and (y) directions, and the capacity curves are obtained as shown in Figure 4.8 and Figure 4.9, respectively.

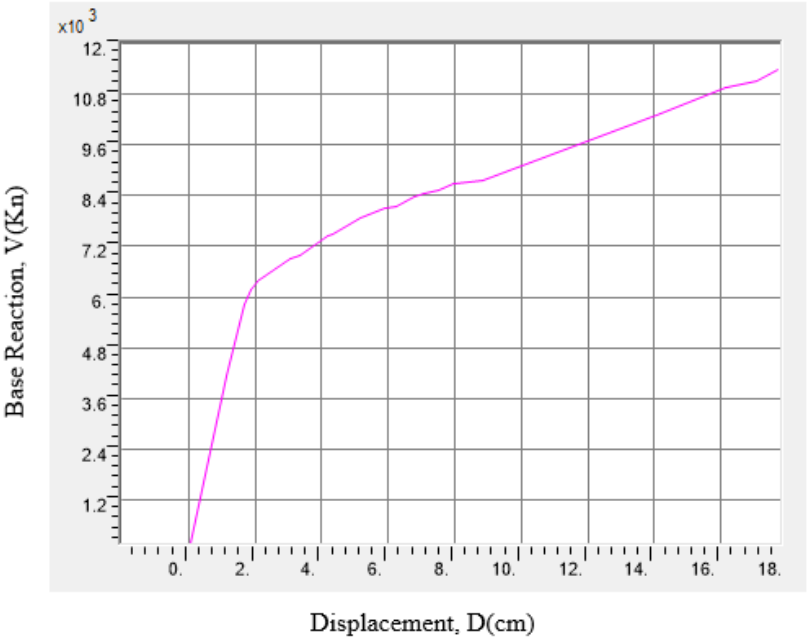

Figure 4.8. Capacity curve for x-direction

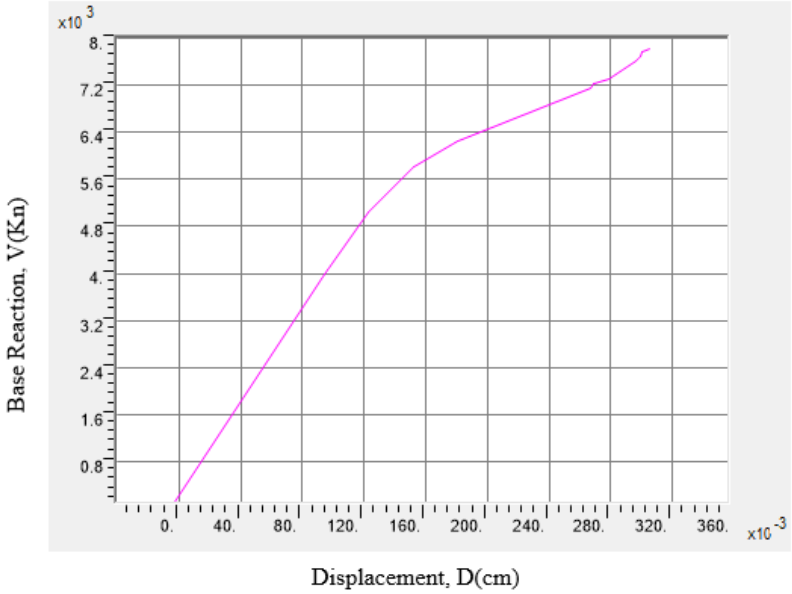

Figure 4.9. Capacity curve for y-direction

As illustrated in Figure 4.8 and Figure 4.9, the capacity curve for y-direction shows more elasticity properties, however the capacity curve for x-direction is turned into plastic stage. Therefore x-direction is considered the critical condition for the structure and the upcoming procedure of the study is done based on the results obtained from the pushover analysis of x-direction.

The aforementioned capacity curve for x-direction is converted into acceleration displacement response spectrum (Figure 4.10.), then the median spectral displacement values are used for obtaining fragility curves which is discussed in the following sections.

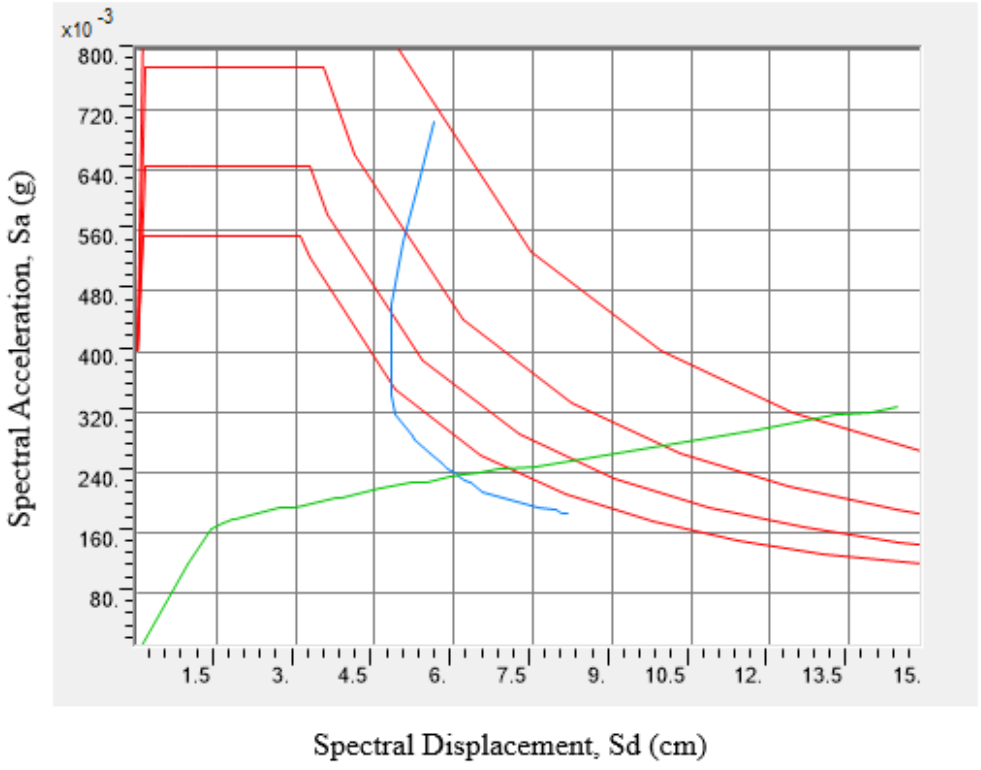

Figure 4.10. Acceleration displacement response spectrum

Where the curve in red color is called demand spectrum, curve in blue color is the demand curve and curve in green color is called the capacity curve. Intersection point of the demand curve and capacity curve is called performance point (Alashker, 2015). The performance points for (V, D) and (Sa, Sd) are shown in Table 4.7.

Table 4.7. Performance points of the structure

Performance points of the structure			
V (kN)	**D (cm)**	**Sa (g)**	**Sd (cm)**
8440.06	7.01	0.236	6.087

4.6 Performance Levels

The plastic hinges are assigned to both ends of the structural elements (Beams & Columns), for columns (P-M2-M3) and for beams (M3) type hinges are assigned as shown in Figure 4.11 and Figure 4.12.

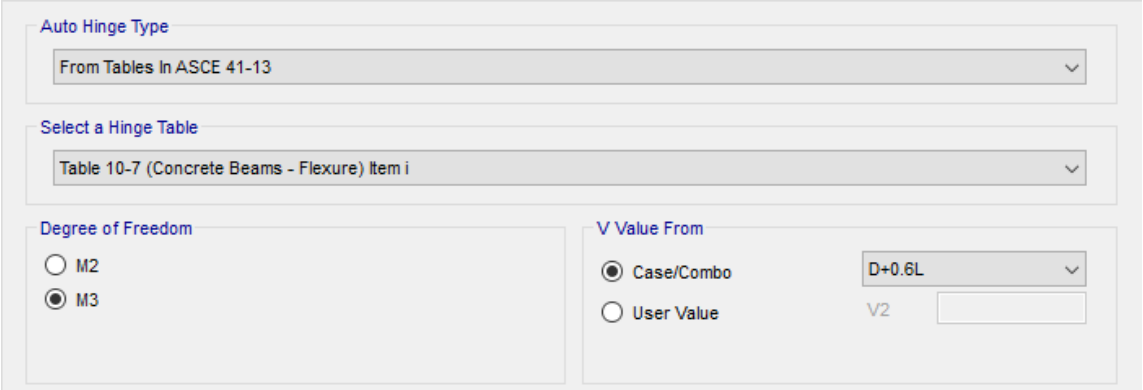

Figure 4.11. (M3) Hinges assigned to beams

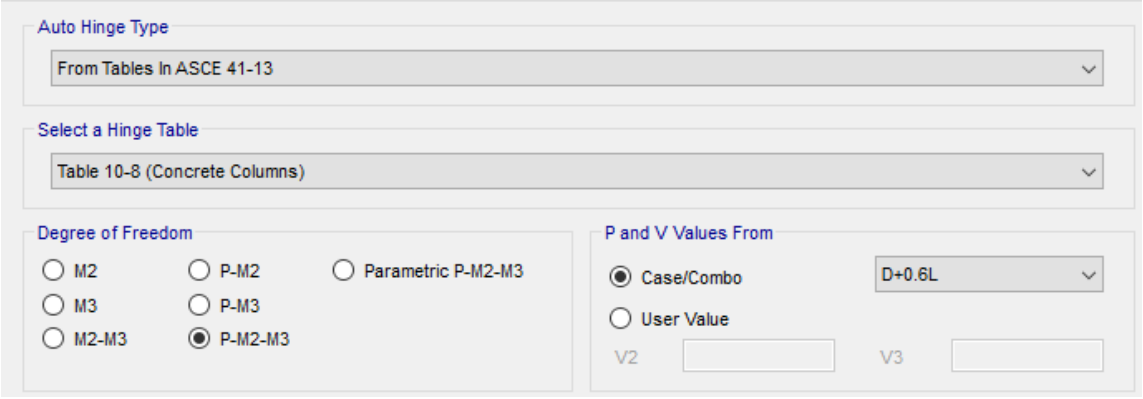

Figure 4.12. (P-M2-M3) Hinges assigned to columns

The significant pushover steps and performance levels of the plastic hinges are shown in Figure 4.13-Figure 4.21.

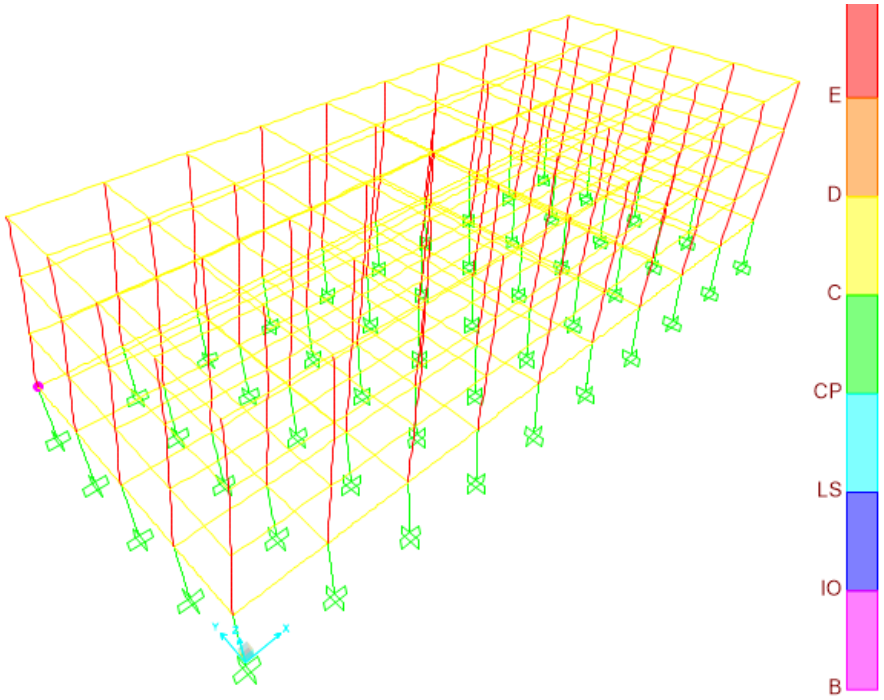

Figure 4.13. Hinge deformation after first pushover step

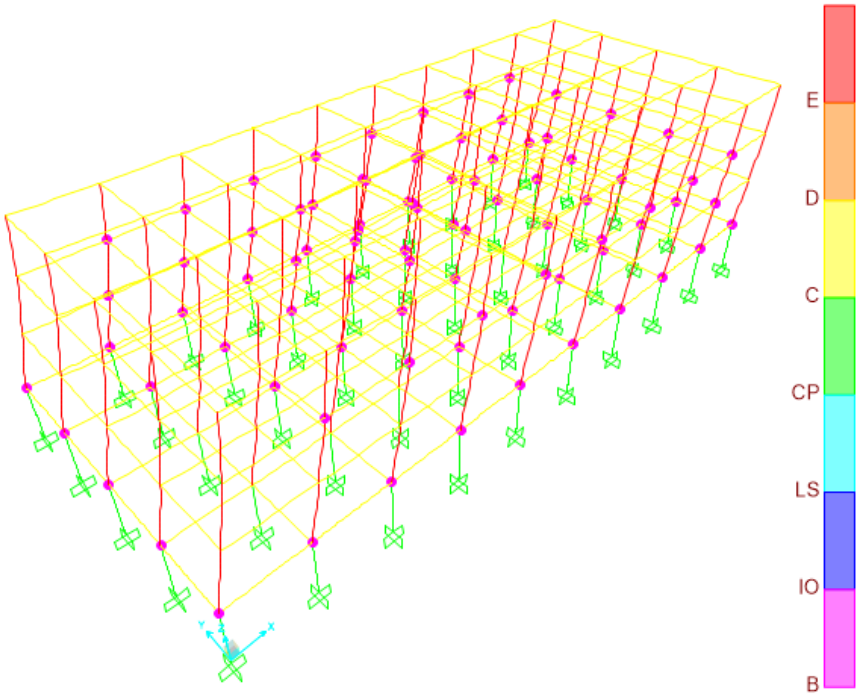

Figure 4.14. Hinge deformation after fourth pushover step

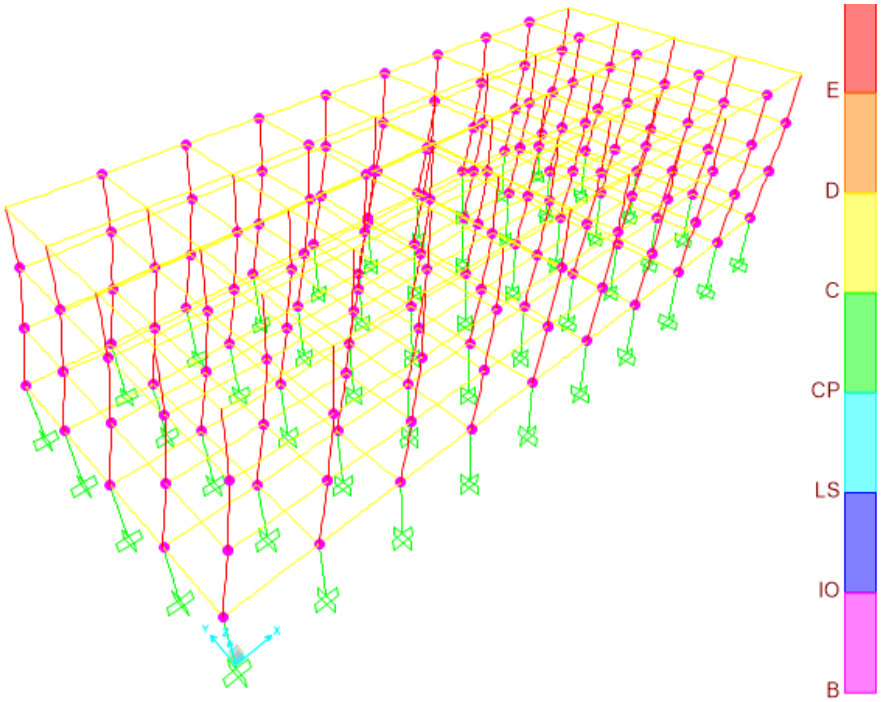

Figure 4.15. Hinge deformation after sixth pushover step

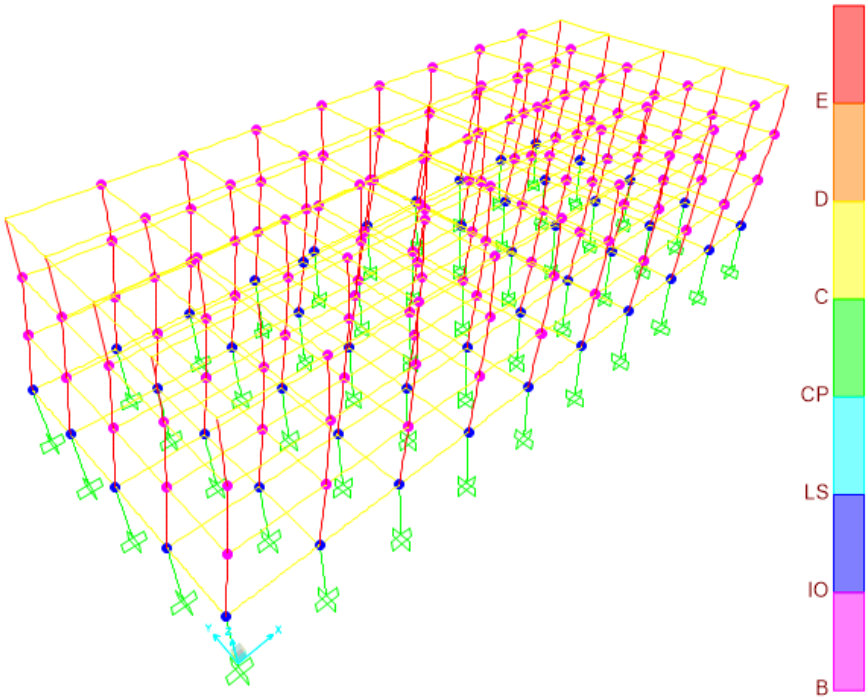

Figure 4.16. Hinge deformations after eighth pushover step

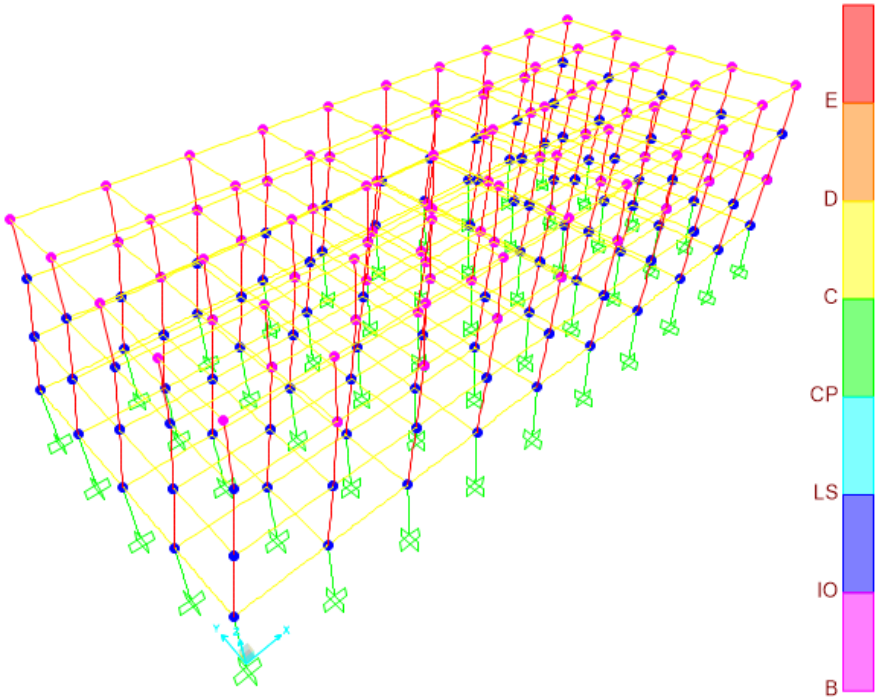

Figure 4.17. Hinge deformations after twelfth pushover step

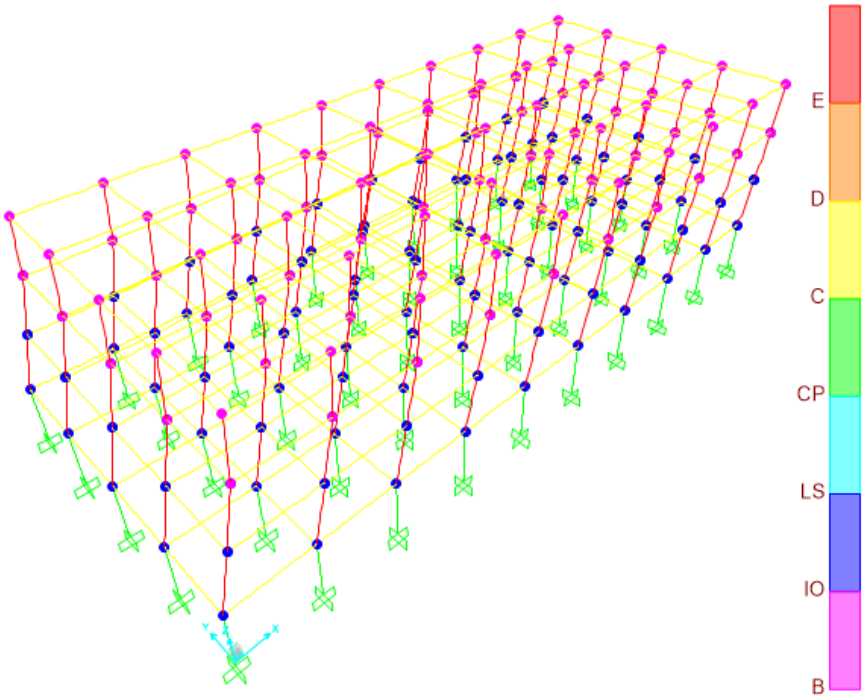

Figure 4.18. Hinge deformations after fourteenth pushover step

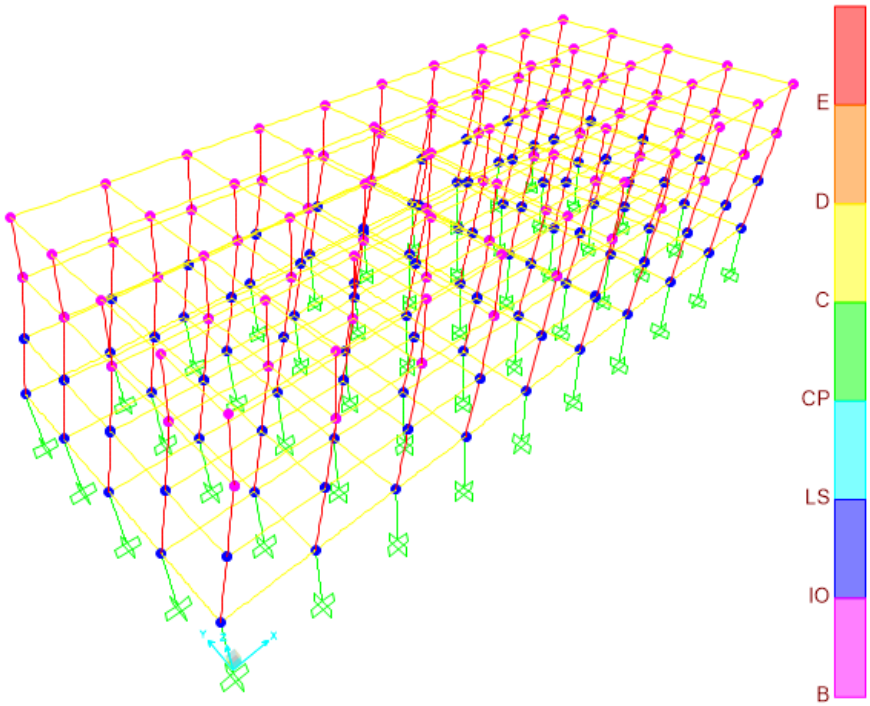

Figure 4.19. Hinge deformations after sixteenth pushover step

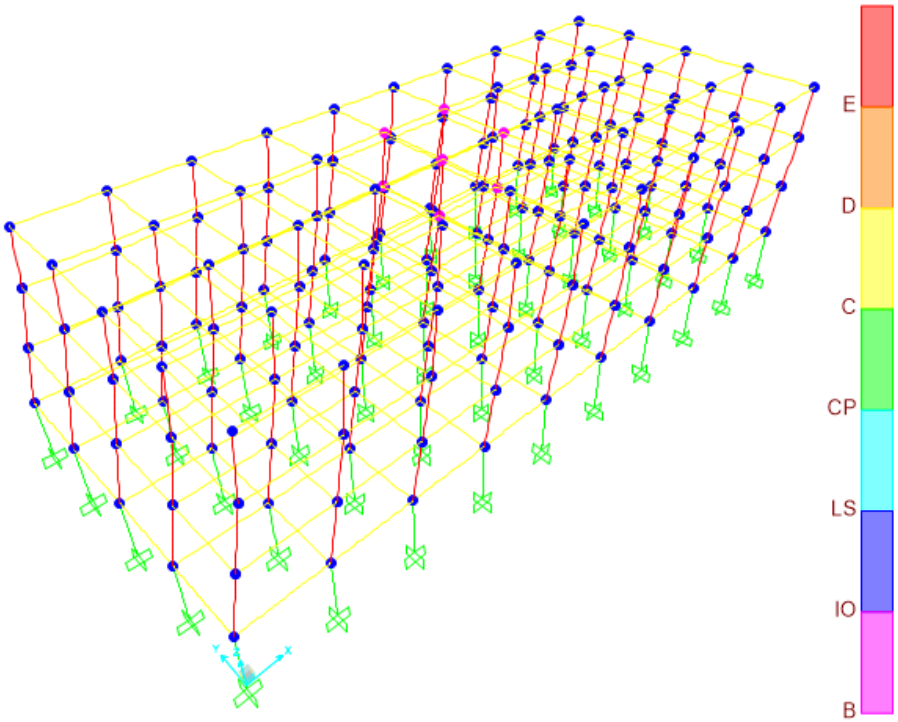

Figure 4.20. Hinge deformations after eighteenth pushover step

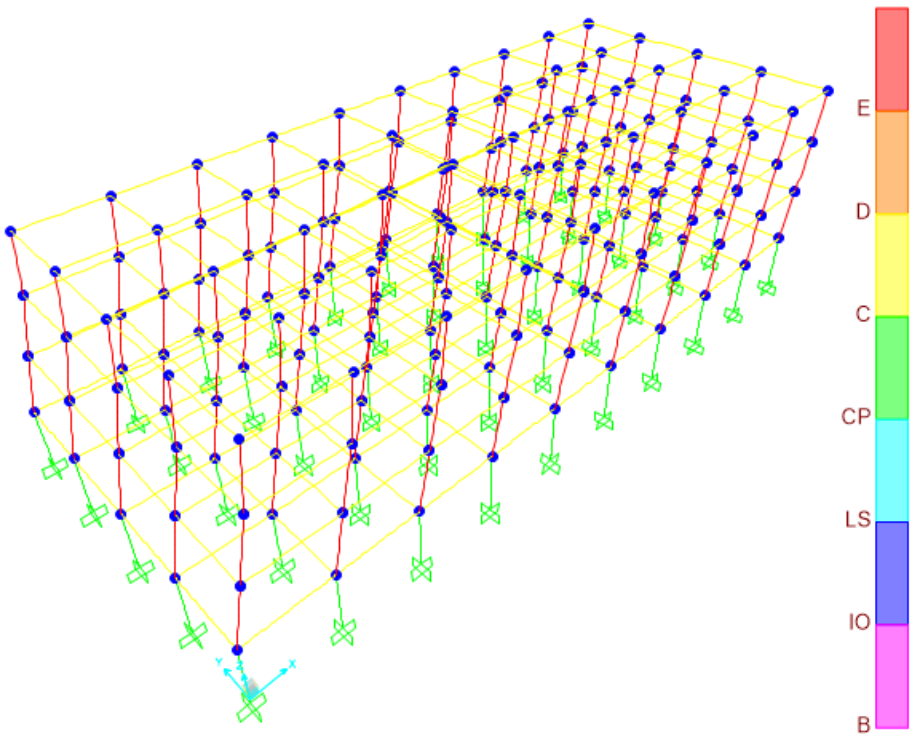

Figure 4.21. Hinge deformations after the last pushover step

4.7 Fragility Analysis

Fragility curves of the structure is obtained using equation (3.3) which is mentioned and explained in the previous pages. First, it is necessary to obtain the $(\bar{S}_{d,}ds)$ and (β_{ds}) values. (β_{ds}) takes different values for every damage state and can be taken directly from HAZUS based on the building types explained by HAZUS and degradation factors (kappa factor, k). According to HAZUS building modeling types, the structure involves in reinforced concrete low-rise building groups (C1L). Similarly, the $(\bar{S}_{d,}ds)$ value changes for every damage state as well.

In this study, degradation factors are selected according to the damage states. For slight damage state minor degradation (k=0.9), for moderate damage state major degradation (k=0.5), for extreme and collapse damage states extreme degradation (k=0.1) is assumed (Vasavada, 2016). The related (β_{ds}) values are described in Table 4.8.

Table 4.8. (β_{ds}) **values (HAZUS-MH-MR5)**

Damage state (ds)	(β_{ds})
Slight	0.7
Moderate	0.85
Extreme	0.95
collapse	0.95

($\bar{S}_{d,}ds$) is a function of yield displacement (S_{dy}) and ultimate displacement (S_{du}). Researchers have been trying to present appropriate models for obtaining median values of spectral displacements. In this study, fragility curves are derived by using the three models which are proposed by Giovinazzi (2005), Barbat et al. (2006), Kappos et al. (2006) and are shown in Table 4.9.

Table 4.9. Models for obtaining ($\bar{S}_{d,}ds$) **values**

Authors	Models for Median spectral displacement values ($\bar{S}_{d,}ds$)			
	Slight	**Moderate**	**Extreme**	**Collapse**
Giovinazzi, 2005	$0.7S_{dy}$	$1.5S_{dy}$	$0.5(S_{du}+S_{dy})$	S_{du}
Barbat et al., 2006	$0.7S_{dy}$	S_{dy}	$S_{dy}+0.25(S_{du}-S_{dy})$	S_{du}
Kappos et al., 2006	$0.7S_{dy}$	S_{dy}	$2S_{dy}$	S_{du}

As shown in Table 4.9., all models have the same $\bar{S}_{d,}ds$ values for slight and collapse damage states. However, for moderate and extreme damage states each model have different $\bar{S}_{d,}ds$ values. The calculated $\bar{S}_{d,}ds$ values for the case study are listed in Table 4.10.

Table 4.10. Median spectral displacement values ($\bar{S}_{d,}ds$) **for the building**

Authors	Median spectral displacement values ($\bar{S}_{d,}ds$)			
	Slight (mm)	**Moderate (mm)**	**Extreme (mm)**	**Collapse (mm)**
Giovinazzi, 2005	11.813032	25.31364	73.00595	129.13614
Barbat et al., 2006	11.813032	16.87576	44.940855	129.13614
Kappos et al., 2006	11.813032	16.87576	33.75152	129.13614

The fragility curves which are obtained using the aforementioned $\bar{S}_{d,}ds$ values (Table 4.10.) are illustrated in Figure 4.22, Figure 4.23, and Figure 4.24.

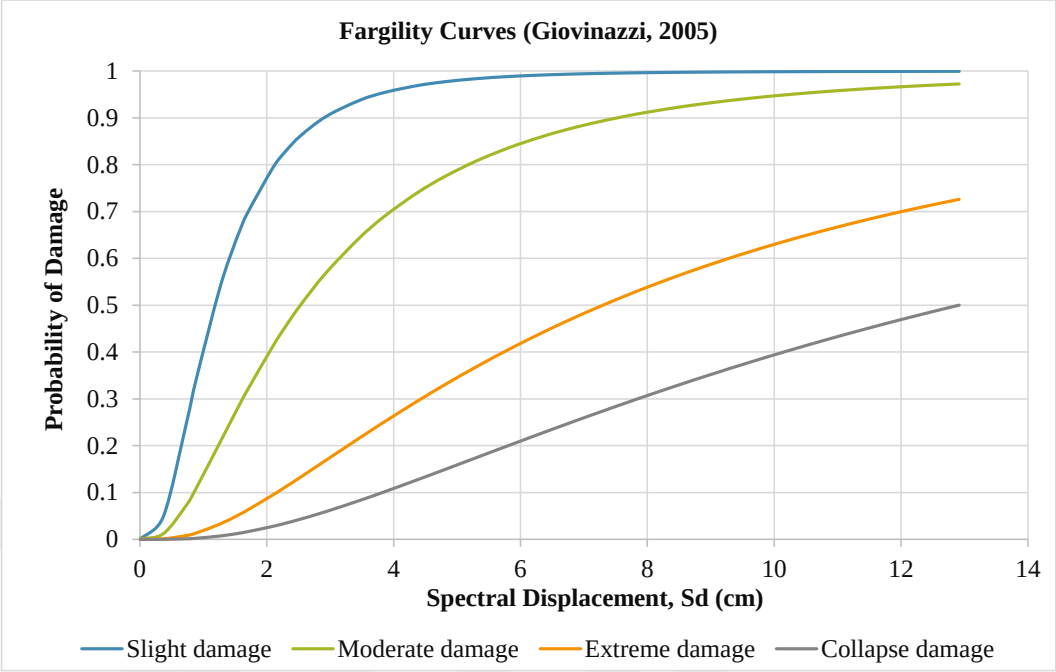

Figure 4.22. Fragility curves based on Giovinazzi (2005), $(\overline{S}_{d,}ds)$ model

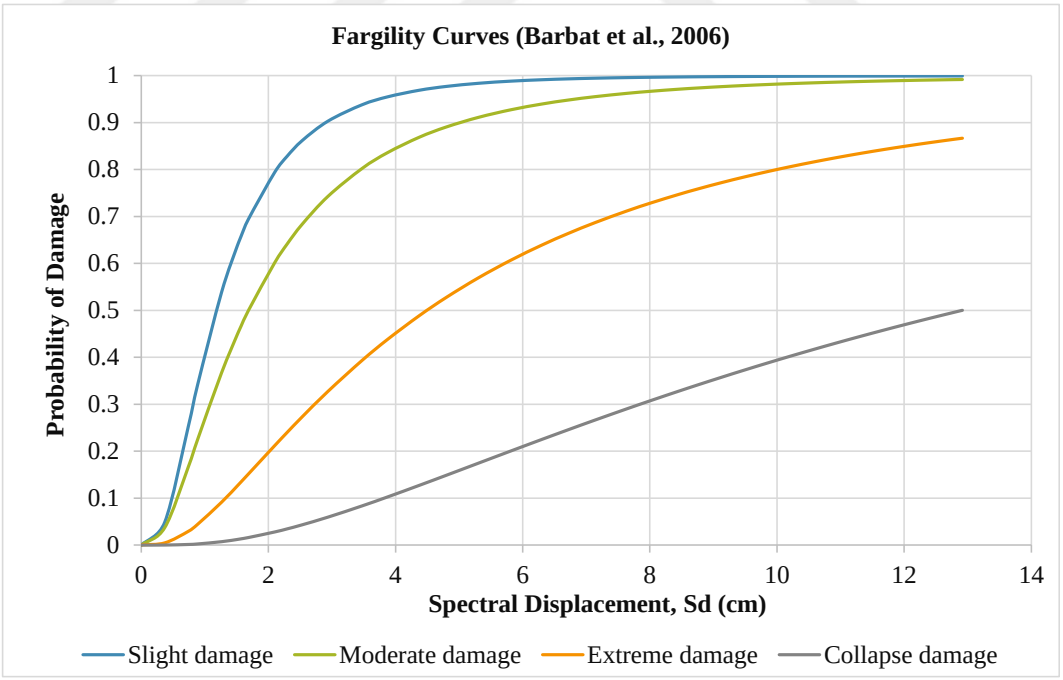

Figure 4.23. Fragility curves based on Barbat et al. (2006), $(\overline{S}_{d,}ds)$ model

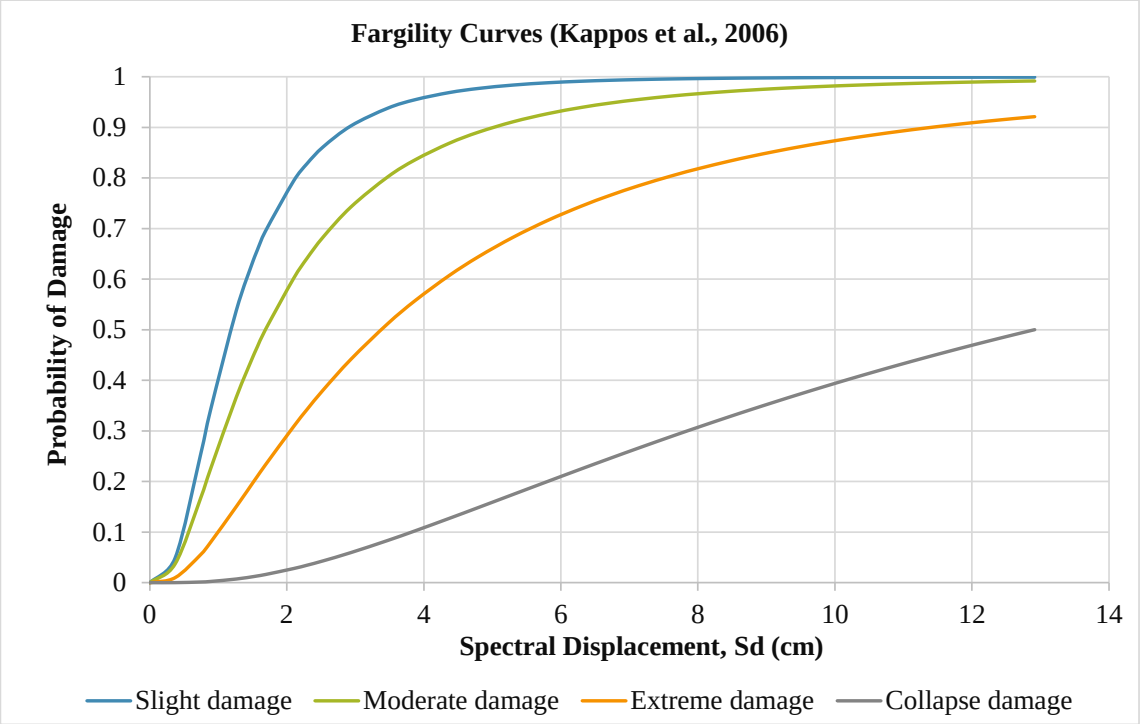

Figure 4.24. Fragility curves based on Kappos et al. (2006), $(\overline{S}_{d,}ds)$ model

It can be seen from the aforementioned fragility curves that, the probability of slight and collapse damage levels are the same in all three types of the fragility curves. But there is an increase of damage probability in moderate and extreme damage levels (Figure 4.23.) and (Figure 4.24.). Especially, the fragility curves obtained using Kappose et al. (2006) model which has a significant increase of damage probability in the extreme damage level (Figure 4.24.). Summary of the damage probabilities that occurs at maximum displacement are listed in Table 4.11.

Table 4.11. Maximum damage probability of each model

Damage state	Maximium Damage probability (%)		
	Giovinazzi (2005)	Barbat et al. (2006)	Kappos et al. (2006)
Slight	99.9	99.9	99.9
Moderate	97.23	99.167	99.167
Extreme	72.6	86.67	92.11
Collapse	50	50	50

4.8 Seismic Loss

Vulnerability curves can be obtained directly from the fragility curves by using equation (3.4) and values listed in Table 2.3 which involves the mean damage factor (MDF) values. Since the fragility curves is obtained for three different conditions according to the proposed models, three different vulnerability curves is determined as well. Figure 4.25. shows the vulnerability curve obtained based on the fragility curves that are illustrated in Figure 4.22, and the maximum damage (%) that the structure will have is listed in Table 4.12.

Table 4.12. Possible maximum damage (%)

Damage (%)		
Giovinazzi (2005)	**Barbat et al. (2006)**	**Kappos et al. (2006)**
63.8	69.6	71.77

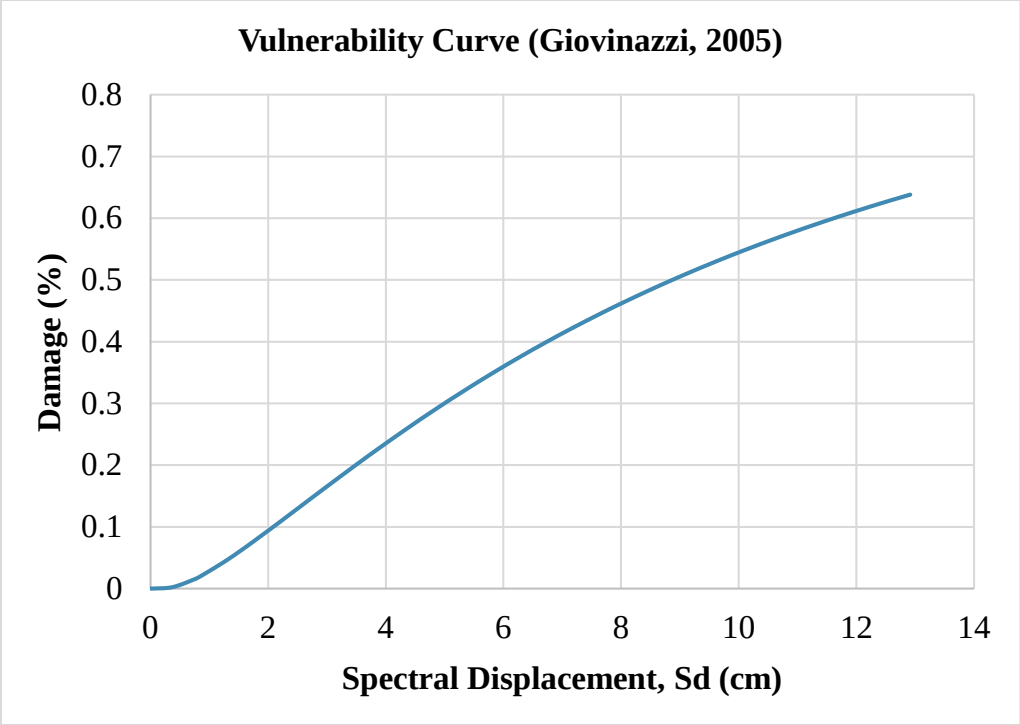

Figure 4.25. Vulnerability curve based on fragility curves obtained by using Giovinazzi (2005)

In the similar way, the other vulnerability curves are obtained and are shown in Figure 4.26 and Figure 4.27.

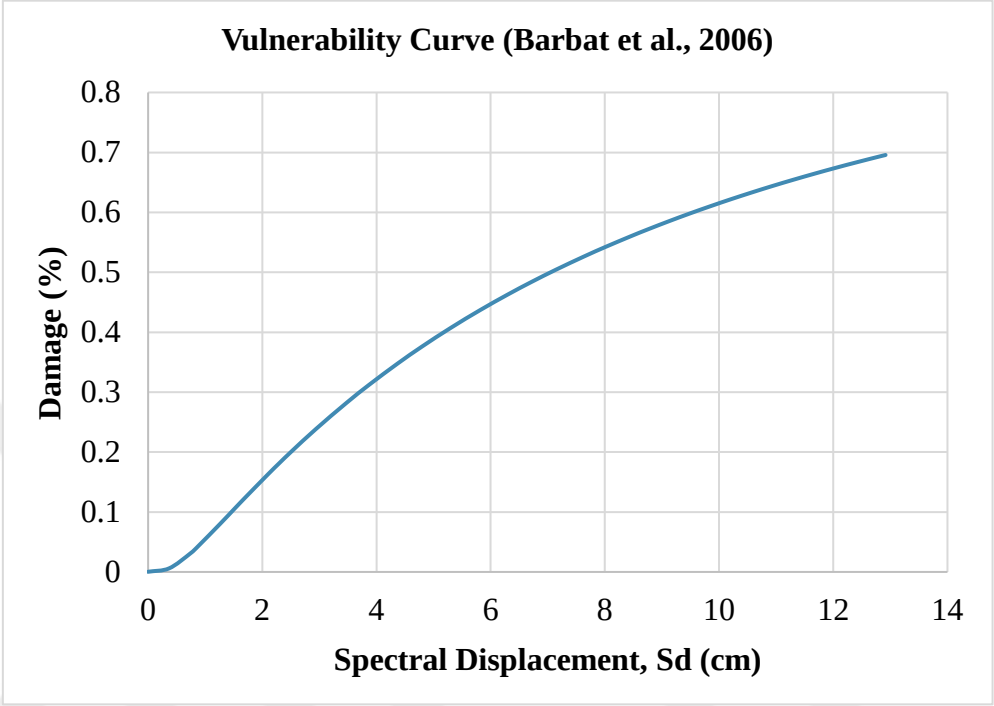

Figure 4.26. Vulnerability curve based on fragility curves obtained by using Barbat et al. (2005)

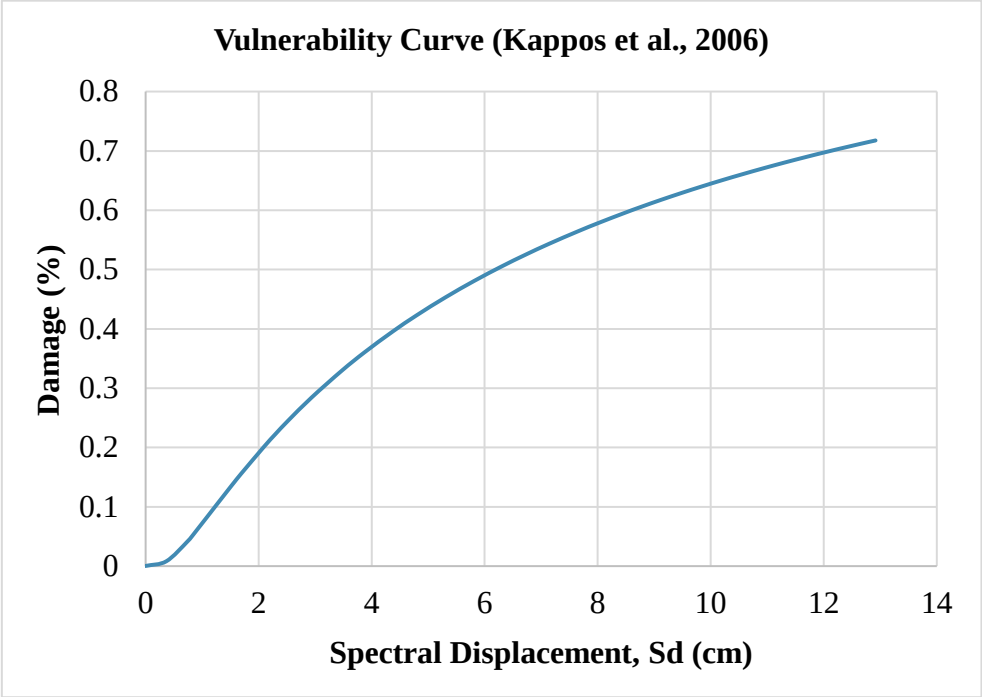

Figure 4.27. Vulnerability curve based on fragility curves obtained by using Kappos et al. (2005)

4.8.1 Comparison of the results

As it is illustrated in Figure 4.28, each vulnerability curve has a different damage level. The lowest damage (%) is obtained from the vulnerability curve based on Giovinazzi (2005). On the contrast, the highest damage (%) is obtained from vulnerability curve based on Kappos et al. (2006). Therefore, it is the critical condition for the building. The resilience procedure will be continued based on that vulnerability curve.

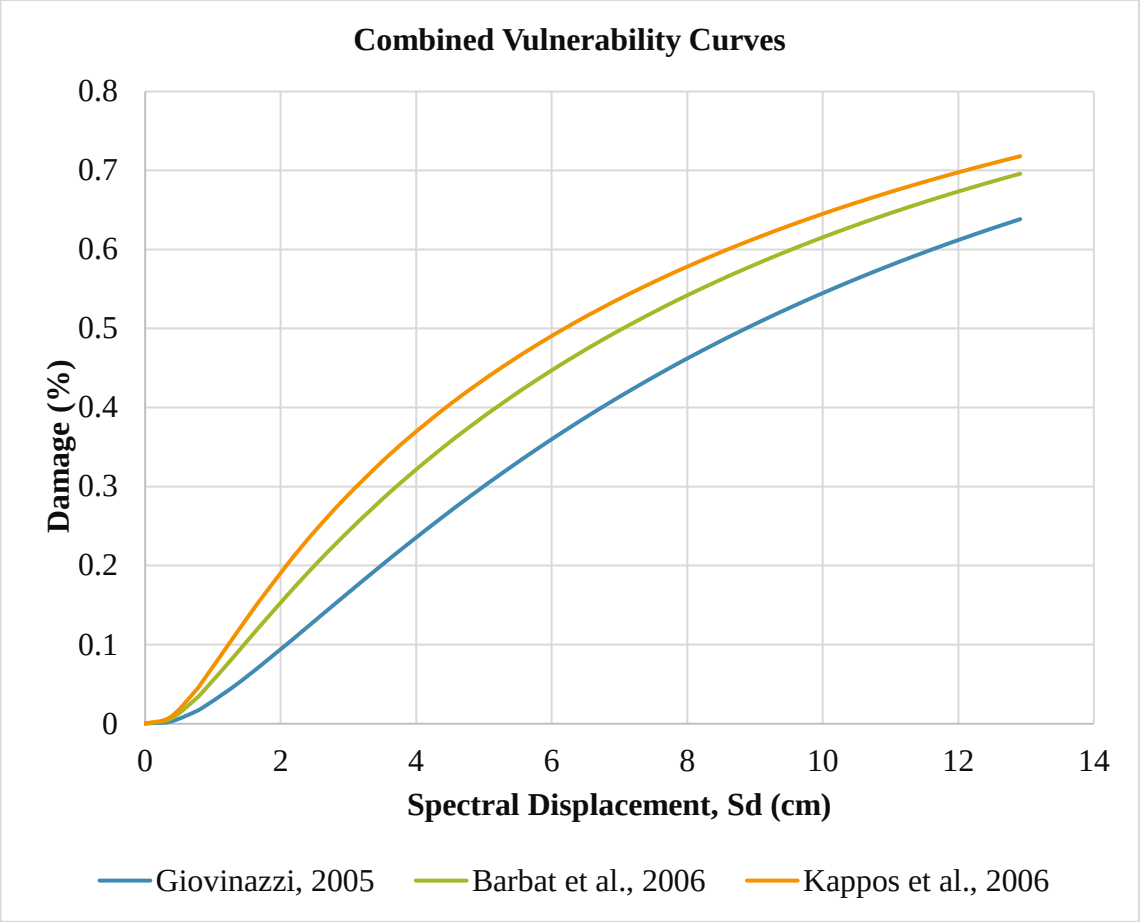

Figure 4.28. Comparison of the results (combination of the vulnerability curves)

4.9 Seismic Resilience of the structure

Last part of the study is the analysis of the resilience. It is obtained by using equation (3.9) which is a combination of three equations: loss function, recovery function and Heaviside function. In this case study, the resilience curve is obtained taking into consideration only the structural damages (direct damages) that occurred in the structure due to a seismic activity. As mentioned in the previous pages, the recovery function has three types, and the resilience curve will be obtained according to each function. Therefore, we will have three different resilience curves. The important parameters of the recovery function are event and recovery times. Selecting the recovery time is one of the complex issues. Generally, the schools in Turkey are reconstructed in 6-10 months, therefore in this study the recovery time is assumed to be taken as 300 days.

To get loss functionality of the structure, it is necessary to understand the damage (%), depreciation and annual discount rates, and $\left(\frac{C_{S,J}}{I_S}\right)$ ratio. The damage (%) is taken directly from vulnerability curves. The maximum damage is obtained (72%) as a result of these vulnerability curves. In this study, depreciation and annual discount rates are assumed to be 2% and 10%, respectively. $\left(\frac{C_{S,J}}{I_S}\right)$ ratio is one of the important parts of the loss functionality which have significant effects on the functionality value. Increase in the $\left(\frac{C_{S,J}}{I_S}\right)$ ratio causes the decrease in the functionality of structure (functionality loss increases). In this case study, three different $\left(\frac{C_{S,J}}{I_S}\right)$ ratios (0.25, 0.35, 0.45) are assumed and finally using equation (3.14), the loss functionality is obtained for three different conditions (Table 4.13).

Table 4. 13 Loss functionality of the structure for different $\left(\frac{C_{S,J}}{I_S}\right)$ values

$\left(\frac{C_{S,J}}{I_S}\right)$	Loss functionality (L_D)
0.25	0.22
0.35	0.31
0.45	0.4

The resilience curves obtained for each $\left(\frac{C_{SJ}}{I_S}\right)$ ratio is shown in Figure 4.29 to:

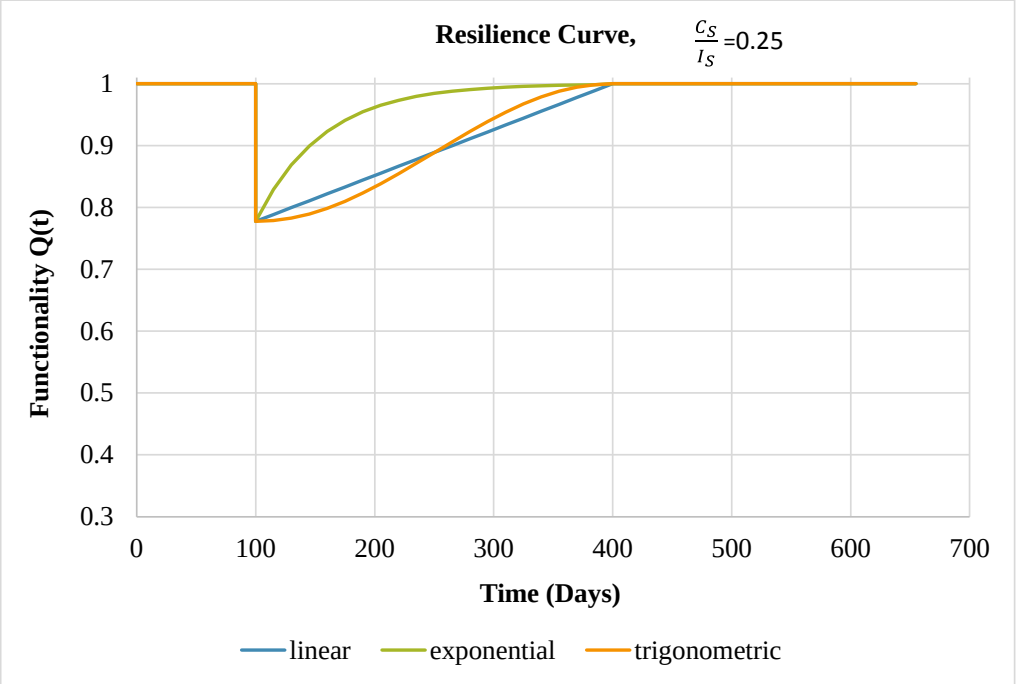

Figure 4.29. Resilience curve of the building $\left(\frac{C_{SJ}}{I_S} = 0.25\right)$

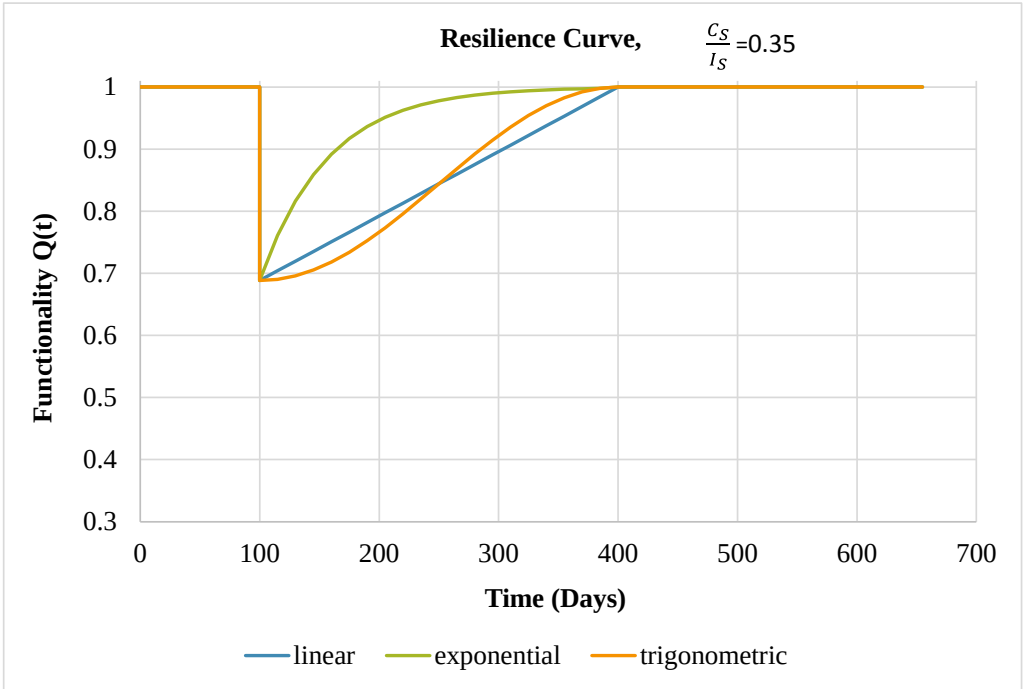

Figure 4.30. Resilience curve of the building $\left(\frac{C_{SJ}}{I_S} = 0.35\right)$

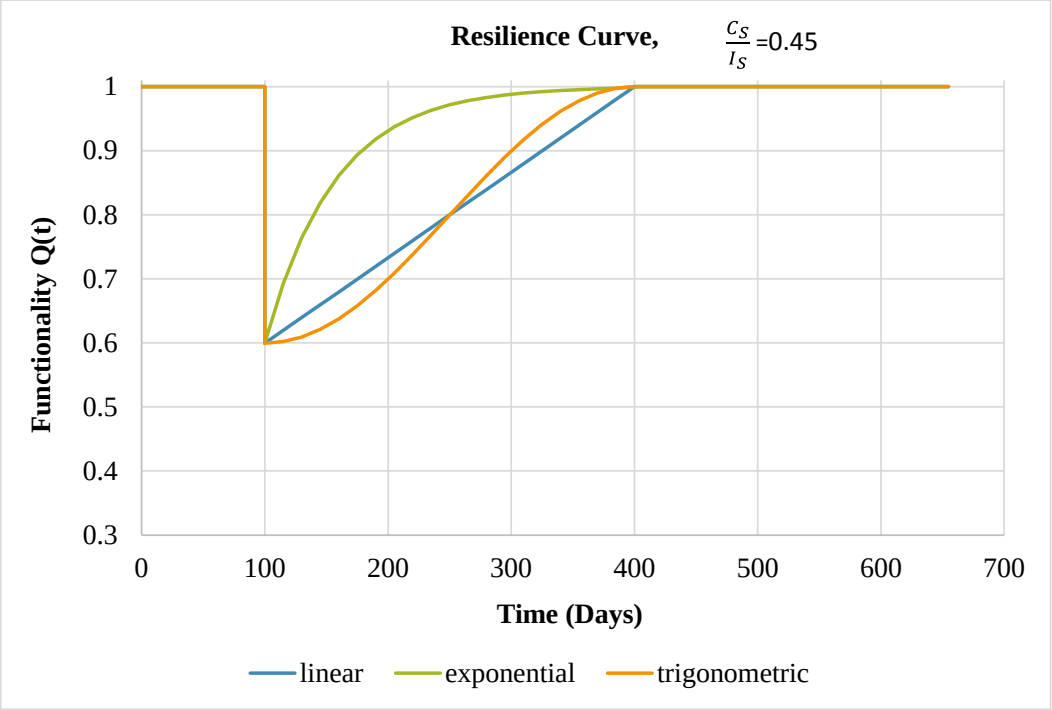

Figure 4.31. Resilience curve of the building $\left(\frac{C_{SJ}}{I_S} = 0.45\right)$

As illustrated in Figure 4.29-Figure 4.31, it can be seen clearly that there is a significant difference in loss functionality. The loss functionality increases from 22% to 40%.

5. CONCLUSIONS

In this thesis, damage assessment (fragility curves, vulnerability curves) and resilience of a RC school building is presented using nonlinear static pushover analysis and the HAZUS methodology. Three different methods based on Giovinazzi (2005), Barbat et al. (2006) and Kappos et al. (2006) to obtain the median spectral displacement $(\bar{S}_{d,}ds)$ values for fragility curves are used. The $(\bar{S}_{d,}ds)$ values obtained for slight and collapse damage states are the same for all three models. Thus, there is no difference in the damage probabilities of these two damage states, as well. However, the values obtained for moderate and extreme damage states differ. Therefore, all three models give three different damage probabilities for moderate and extreme damage states. The fragility curves obtained by using Kappos et al. (2006) model shows the highest damage probabilities with respect to the other two models. As a result, the vulnerability curve obtained according to Kappos et al. (2006) has the highest damage (%) which is used for seismic resilience curve. In addition, the study concluded that $\left(\frac{C_{S,J}}{I_S}\right)$ ratio and recovery time (T_{RE}) have significant effects on the rapidity of reconstruction or repairing of the structure. Despite that, the $\left(\frac{C_{S,J}}{I_S}\right)$ effects the loss functionality of the structure, as well. As it is observed, increase in the $\left(\frac{C_{S,J}}{I_S}\right)$ ratio causes increase in the loss functionality, as well. All in all, the important factors that effect the resilience curve are $\left(\frac{C_{S,J}}{I_S}\right)$ ratio, $(\bar{S}_{d,}ds)$ values, recovery time and seismic damage (%) or vulnerability curve. Consequently, this study will form a basis for the resilience analysis of the school buildings in Turkey.

REFERENCES

Alashker,Y., Nazar, S., and Ismaiel, M. (2015). Effects of Building Configuration on Seismic Performance of RC Buildings by Pushover Analysis. *Open Journal of Civil Engineering*, 5, 203-213.

Barbat,A.H., Pujades,L.G., and Lantada, N. (2006). Performance of Buildings under Earthquakes in Barcelona, Spain. *Computer-Aided Civil and Infrastructure Engineering*, 21, 573–593.

Bruneau, M., Chang, S. E., Eguchi, R. T., Lee, G.C., O'Rourke, T. D., Reinhorn, A. M., Shinozuka, M., Tierney, K., Wallace, W. A., and Winterfeldt, D.V. (2003). A framework to quantitatively assess and enhance the seismic resilience of communities. *Earthquake Spectra*, 19, 733–752.

Bruneau.M., and Reinhorn.A. (2004). Seismic Resilience of Communities – Conceptualization and Operationalization, 19, 733-752.

Burton, H. V., Deierlein,G., Lallemant,D., and Singh,Y. (2017). Measuring the Impact of Enhanced Building Performance on the Seismic Resilience of a Residential Community. *Earthquake Spectra*, 33, 1347–1367.

Cimellaro,P. G., Reinhorn, A., and Bruneau, M. (2005). Seismic Resilience of a Health care facility. In Proceedings of the 2005 ANCER Annual Meeting, Session III, November 10–13, Jeju, Korea.

Cimellaro,P. G., Reinhorn, A.M, and Bruneau, M. (2010). Seismic resilience of a hospital system. *Structure and Infrastructure Engineering*, 6, 127-144.

Disaster and Emergency Management (AFAD).
(https://tdth.afad.gov.tr/TDTH/main.xhtml)

General Directorate of Mineral Research and Exploration (MTA).
http://yerbilimleri.mta.gov.tr/anasayfa.aspx

Giovinazzi, S. (2005). The Vulnerability Assessment and the Damage Scenario in Seismic Risk Analysis. (Doctoral Dissertstion, Technical University of Braunschweig). *Braunschweig university library.*

González, C., Niño, M., and Jaimes, MA. (2020). Event‐based assessment of seismic resilience in Mexican school buildings. *Bulletin of Earthquake Engineering.* 18:6313–6336.

Grünthal, G. (editor). (1998). European Macroseismic Scale 1998. European Seismological Commission, subcom-mission on Engineering Seismology. Volume: 15, Luxembourg 1998.

Güler, K., and Celep, Z. (2020). On the general requirements for design of earthquake resistant buildings in the Turkish Building Seismic code of 2018. *IOP Conference Series: Materials Science and Engineering* **737** (2020) 012015.

Hamadamin, S.S. (2014). Pushover Analysis and Incremental Dynamic Analysis of Steel Braced Reinforced Concrete Frames. (Thesis,M.Sc). *Eastern Mediterranean University, Institute of Graduate Studies and Research, Dept. of Civil Engineering, Famagusta: North Cyprus.*

HAZUS Technical Manual (2003). Multi-hazard Loss Estimation Methodology. *National Institute of Building Sciences Washington, D.C.*

HAZUS technical and user's manual MH-MR-5, Earthquake loss estimation methodology, Department of homeland security and Federal Emergency Management Agency, Washington DC, USA.

İnce, G.Ç., and Yılmazoğlu, M.U. (2021). Probabilistic seismic hazard assessment of Muğla, Turkey. *Natural Hazards.* 107, 1311-1340.

Kappos, A.J., Panagopoulos, G., Panagiotopoulos, C., and Penelis, G. (2006). A hybrid method for the vulnerability assessment of R/C and URM buildings. *Bull Earthquake Eng,* 4:391–413.

Motlagh,Z.S., Dehkordi,M.R.,Eghbali,M., and Samadian,D. (2020). Evaluation of seismic resilience index for typical RC school buildings considering carbonate corrosion effects. International Journal of Disaster Risk Reduction. 46, p. 101511.

Prasanth,S., and Ghosh, G. (2020). Effect of variation in design acceleration spectrum on the seismic resilience of a building. *Asian Journal of Civil Engineering.* 22, 331-339

Sadeghi, M., Ashtiany, M.G., and Lahiji, N.P. (2015). Developing seismic vulnerability curves for typical Iranian buildings. *Proc IMechE Part O: J Risk and Reliability.* vol. 229, no. 6, pp. 627–640.

Samadian, D., Ghafory-Ashtiany, M., Naderpour, H., and Eghbali, M. (2019). Seismic resilience evaluation based on vulnerability curves for existing and retrofitted typical RC school buildings. *Soil Dynamics and Earthquake Engineering,* 127, p. 105844.

Sardari,F., Dehkordi,M.R., Eghbali,M., and Samadian,D. (2020). Practical seismic retrofit strategy based on reliability and resiliency analysis for typical existing steel school buildings in Iran. *International Journal of Disaster Risk Reduction.* 51, p. 101890.

Vasavada, M., and Patel, V.R. (2016). Development of Fragility Curves for RC Buildings using HAZUS method. *International Research Journal of Engineering and Technology (IRJET)*, Volume: 03, Issue: 05, 2256 – 2262.

Xiong, C., Huang, J., and Lu, X. (2020). Framework for city-scale building seismic resilience simulation and repair scheduling with labor constraints driven by time–history analysis. *Comput Aided Civ Inf*. 2020; 35:322–341.

CURRICULUM VITAE

Personal Information

Name Surname : Z****r S****i

Nationality : AFGHAN

Date and place of Birth : 03/07/1994, Afghanistan, Wardak

E-mail : z*******2@gmail.com

EDUCATİON

Degree	Institution	Year
High School	Saidabad High School	2010-2013
B. S	Yıldız Technical University Department of Civil Engineering	2013-2019
M.Sc	Muğla Sıtkı Koçman University Department Civil Engineering.	2019-2021

Work Experience

Year	Place	Employment
2018-2019	EMCO İnşaat	Civil Engineer

Foreign Languages

English (Advance), Turkish (Intermediate), Persian (Advance), Pashto (Native)

Skills

Computer Programs-Languages:

Microsoft Office : Good

Sap2000 : Excellent

MatLAB : Good

OpenSees : Intermediate